HHS Public Access

Author manuscript

Cancer Immunol Res. Author manuscript; available in PMC 2020 August 16.

Published in final edited form as:

Cancer Immunol Res. 2019 October ; 7(10): 1647–1662. doi:10.1158/2326-6066.CIR-18-0934.

MicroRNA *Mirc11* optimizes the inflammatory responses by silencing ubiquitin modifiers and altering K63 and K48 ubiquitylation of TRAF6

Arash Nanbakhsh[1], **Anupallavi Mani**[1], **Sandra Holzhauer**[2], **Matthew Riese**[2,6,7], **Yongwei Zheng**[3], **Demin Wang**[3,7], **Robert Burns**[4], **Michael H Reimer**[5,8], **Sridhar Rao**[5,8], **Angela Lemke**[9,10], **Shirng-Wern Tsaih**[9,10], **Michael J Flister**[9,10], **Richard Dahl**[12], **Shunhua Lao**[1,11], **Monica S Thakar**[1,11], **Subramaniam Malarkannan**[1,6,7,9,11]

[1]Laboratory of Molecular Immunology and Immunotherapy, Blood Research Institute, BloodCenter of Wisconsin, Milwaukee, WI

[2]Laboratory of Lymphocyte Signaling, Blood Research Institute, BloodCenter of Wisconsin, Milwaukee, WI

[3]Laboratory of B cell Biology, Blood Research Institute, BloodCenter of Wisconsin, Milwaukee, WI

[4]Bioinformatics Core, Blood Research Institute, BloodCenter of Wisconsin, Milwaukee, WI

[5]Laboratory of Stem Cell Biology, Blood Research Institute, BloodCenter of Wisconsin, Milwaukee, WI

[6]Department of Medicine, Medical College of Wisconsin, Milwaukee, WI

[7]Department of Microbiology and Immunology, Medical College of Wisconsin, Milwaukee, WI

[8]Department of Cell Biology, Medical College of Wisconsin, Milwaukee, WI

[9]Genome Sciences and Precision Medicine Center, Medical College of Wisconsin, Milwaukee, WI

[10]Department of Physiology, Medical College of Wisconsin, Milwaukee, WI

[11]Department of Pediatrics, Medical College of Wisconsin, Milwaukee, WI

[12]Indiana University School of Medicine, South Bend, IN

Abstract

Proinflammatory cytokines produced by lymphocytes are required to contain tumor growth. Post-transcriptional mechanisms that regulate this process remains unknown. Here, we identify that the microRNA cluster *Mirc11* is a central regulator of NK cell-mediated proinflammatory responses.

Correspondence should be addressed to S.M. (subra.malar@bcw.edu).

Author contributions.

A.N. performed the experiments and processed the data. A.M., S.H., A.L., and S.L. contributed in part with performing experiments. M.H.R. helped with performing NextSeq experiments. Y.Z. and D.W. helped to perform the Gel-Shift analyses. S-W.T. and M.J.F. analyzed and processed the transcriptomic data. R.B. helped in part by analyzing the transcriptomic data. M.R., S.R., M.S.T. contributed towards planning the experiments and editing of the manuscript. R.D. contributed reagents. S.M. conceived the concept, designed experiments, wrote the manuscript.

Competing Statement: All the authors hereby declare that there is no competing statement with the work performed, analyzed, and presented in this manuscript.

The absence of *Mirc11* only moderately reduced NK cell-mediated anti-tumor cytotoxicity. However, the loss of *Mirc11* significantly reduced the generation of proinflammatory cytokines *in vitro* and the Interferon-γ-dependent clearance of B16F10-melanoma or *Listeria monocytogenes in vivo* by NK cells. We define *Mirc11* optimizes inflammatory cytokine production by silencing the translation of ubiquitin modifiers A20, Cbl-b and Itch, allowing TRAF6-dependent activation of NF-κB and AP-1. A lack of *Mirc11* caused an increased translation of A20, Cbl-b, and Itch proteins, resulting in the deubiquitylation of scaffolding K63 and the addition of degradative K48 moieties on TRAF6. Our results provide a novel mechanism by which *Mirc11* fine tunes NF-κB and AP-1-dependent cytokine gene transcriptions and anti-tumor responses.

Introduction

NK cells generate proinflammatory factors and mediate anti-tumor cytotoxicity (1, 2). Upon recognizing target cells expressing pathogen-derived ligands or '*induced-self*' self-antigens through germline-encoded activation receptors including NCR1 and NKG2D, NK cells initiate an array of signaling cascades (3). Adaptor proteins such as DAP10 (4), DAP12 (5–7), and CD3ζ (8) play central role in initiating the phosphorylation and recruitment of key signaling proteins including Syk (9), Fyn (10), Lck (11), PI(3)-p110δ/p85α (12–14), Grb2 (15), PLC-γ2 (16, 17), ADAP (18, 19), PKC-θ (20), Carma1 (21), Bcl10 (22), and TAK1 (23). E3 ligases including TRAF2 and TRAF6 promote K63-linked polyubiquitination that is required for the sub-cellular localization of the substrates (24), and subsequent activation of signaling proteins required for NF-κB (25) and AP-1-mediated gene transcriptions (26). Stringent regulation of these signaling events is central to promote optimal immune responses and to limit uncontrolled inflammation (27). One established mechanism is mediated by lipid (SHIP, PTEN) and protein phosphatases (CD45, SHP1, SHP2) that are recruited to inhibitory Ly49/KIR receptors which block or dampen an ongoing activation event (28–34). In addition to these phosphatases ubiquitin regulators such as A20, Itch, Cbl-b, and Cyld synthesize and add polyubiquitin chains via lysine (K) 48 of ubiquitin molecules leading to the proteasomal degradation of the substrates (35–38). Ubiquitin regulators can alter the threshold and the activation of NF-κB and AP-1 by targeting multiple signaling proteins including TRAF6 (39). While these inhibitory mechanisms have been well-characterized, the role of small non-coding microRNAs (miRNAs), which provides critical repressive functions in other cell types, and their temporal regulation of signaling in NK cells is mostly unknown.

miRNAs are small (~22 nucleotides) non-coding sequence-specific guides that direct Argonaute protein complex, an essential component of the RNA-induced silencing complex (RISC) to silence protein translation by Watson-Crick pairing to mRNA transcripts (40). Mature miRNAs contain a 'seed sequence' of 2 to 8 nucleotides that interact with a sequence of 6 to 8 nucleotides in the 3′ untranslated regions (3′ UTR) of the target mRNAs (41). Binding of miRNAs to target mRNAs results in translational inhibition or transcript degradation (42). The miRNAs are highly conserved among different species (43). Expression of miRNAs is cell-specific, and each cell expresses a different set of miRNAs at various stage of maturation, differentiation or activation (44). While it is clear that miRNAs play essential roles in lymphocyte development, activation and effector functions, the

mechanism by which miRNA mediate these effects is poorly understood. Genes encoding mammalian miRNAs can be expressed as mono- or polycistronic transcripts (45). *Mirc11* cistron (*miRNA-23a* cluster) is a tri-miRNA cluster that is highly conserved in mouse and human genomes. It consists of three members, *miR-23a*, *miR-27a*, and *miR-24-2*, which are derived from a single primary mRNA transcript (46). The *Mirc22* cistron (*miRNA-23b* cluster) is a paralog of *Mirc11* cistron and is made up of *miR-23b*, *miR-27b*, and *miR-24-1* (46). Despite the recent advances on *Mirc11* cistron in lymphocyte biology (47, 48), there exists minimal functional or mechanistic insight into its role on NK cell development and effector functions.

In this study, we define the *Mirc11* cistron as an obligatory regulator of the inflammatory responses in NK cells. A lack of the *Mirc11* cluster did not affect the development of NK cells. Assessment NK cell-mediated cytotoxicity showed the *ex vivo* and *in vitro* anti-tumor cytotoxic potentials of NK cells from *Mirc11*$^{-/-}$ mice were mostly intact; while, NK cell-mediated *in vivo* rejection of donor splenocytes that lacked the surface expression of MHC Class I ('*missing-self*') was significantly reduced in *Mirc11*$^{-/-}$ mice. Compared to the cytotoxic potential, *in vitro* stimulation of NK cells from *Mirc11*$^{-/-}$ mice with mitogenic antibodies revealed a significant defect in the production of inflammatory cytokines including IFN-γ, GM-CSF, CCL3, CCL4, and CCL5. The link between the *Mirc11* cluster and NK cell-mediated inflammatory responses was validated by the inability of the *Mirc11*$^{-/-}$ mice to mediate NK cell-dependent *in vivo* clearance of *Listeria monocytogenes*.

Moreover, lack of *Mirc11* resulted in defective clearance of pulmonary pseudometastases following injections with B16F10 melanoma. The transcriptome-wide analyses of NK cells following either anti-NKG2D-mediated *in vitro* stimulation or *in vivo* Listeria-challenge indicated a global defect in NF-κB- and AP-1-mediated gene transcription in the absence of the *Mirc11* cluster. Based on these findings, we hypothesized that one or more negative regulators of the activation of NF-κB and AP-1 are the targets of the *Mirc11* cistron. We found that members of *Mirc11* cistron targeted and silenced the transcripts encoding A20, Itch, and Cbl-b, and thereby reducing the TRAF6-mediated activation and nuclear translocation of NF-κB and AP-1 complexes. Reduced TRAF6 activity mediated by *Mirc11* resulted from increased protein translation of A20, Itch, and Cbl-b resulting in decreased K63 ubiquitination and increased degradation of TRAF6. Our findings provide novel insights into the microRNA-mediated regulation of NK cell-mediated effector functions and provide exciting novel targets for containing pathological inflammation.

Results

Lack of *Mirc11* cluster does not alter NK cell development

Mirc11 cluster consists of *miR-23a*, *miR-27a*, and *miR-24-2* (Supplemental Figure 1A) and acts as a switch in regulating the lineage commitment of hematopoietic stem and progenitor cell (HSPC) into either common lymphoid progenitors (CLPs) or common myeloid progenitors (CMP) (49, 50). A lack of *Mirc11* increased the absolute number of CLPs leading to increased numbers of B cells (51). Thus, as a first step, it was necessary to define the role of the *Mirc11* cluster in NK cell development and function. Through the utilization of knockout mice that globally lacked *miR-23a*, *miR-24-2*, and *miR-27a* (*Mirc11 cluster*),

we identified that the total cellularity of the BM and the spleen was comparable between WT and *Mirc11*$^{-/-}$ mice (data not shown). Earlier studies have shown that the process of NK cell development can be defined as distinct stages based on the expression pattern of cell surface markers (52). Percentages of NK cells as defined by CD3ε^{-}NK1.1^{+} staining in the BM and other peripheral organs such as spleen, liver, lung, and blood were also comparable between WT and *Mirc11*$^{-/-}$ mice (Supplemental Figure 1B). Expression of CD122, the β chain of IL-2 and IL-15 receptors which demarcates the commitment of CLPs into NK precursors (NKPs) in the BM (53), and the absolute number of cells expressing CD122 were unaltered in the BM of *Mirc11*$^{-/-}$ mice (data not shown). Expression of NKG2D, NK1.1, and NCR1 that are the earliest known NK cell activating receptors, which marks the transition of NKPs into Stage-A immature NK cells (iNK) (54), along with NKG2A/C/E (Stage-B iNK), were comparable between WT and *Mirc11*$^{-/-}$ mice (data not shown).

To evaluate more mature populations of NK cells, we analyzed the expression of CD51 (α_v) and CD49b, which defines entry of iNKs into mature NK (mNK; Stage-D) cells and observed little difference between *Mirc11*-deficient and replete mice. Populations of NK cells representing functional maturation, as delineated by a decrease in the expression levels of CD51 (Kim et al., 2002) and the expression of CD27, integrin CD11b (αMβ2), and eventually, loss of CD27 were also comparable between mice of the two genotypes (Supplementary Figure 1C, D), as were Stage-E NKs defined by the stochastic acquisition of distinct Ly49 receptors such as Ly49C/I, Ly49H, Ly49A, Ly49D, and Ly49G2 (52) (Supplementary Figure 1C, E). Terminally mature NKs (Stage-F) as defined by KLRG1expression (55) was also unaltered in *Mirc11*$^{-/-}$, relative to WT, mice. Based on these data, we conclude lack of *Mirc11* does not affect the development and maturation of NK cells.

Lack of *Mirc11* moderately impairs NK cell-mediated cytotoxicity

Anti-tumor cytotoxicity is one of the vital effector functions of NK cells. Towards this, we evaluated the cytotoxic potential of naïve NK cells against B16F10 tumor cells that express CD155 (*Induced-self*), a ligand for DNAM-1; parental EL4 thymoma cells (*Self*); EL4 cells stably transfected with H60 (EL4^{H60}), a ligand for NKG2D (*Induced-self*); RMA cells (*Self*); RMA/S cells which lack the normal expression of MHC Class I H-2^{b} (*Missing-self*); and YAC1 cells that are of H-2^{a} strain background (*Allo*). Naïve NK cells were not able to mediate detectable cytotoxicity against B16F10 cells. Cytotoxicity against EL4^{H60} was higher compared to the parental EL4; however, there were no differences between NK cells derived from WT and *Mirc11*$^{-/-}$ mice. Similarly, cytotoxicity against YAC1 cells was not affected by the lack of *Mirc11* complex. However, lack of *Mirc11* complex significantly reduced the cytotoxicity against RMA/S at all E:T ratios (Supplementary Figure 2A).

Earlier studies have shown that IL-2 plays a crucial role in the clearance of B16F10 cells *in vivo* (56). Therefore, we expanded purified splenic NK cells with IL-2 and tested their cytotoxic potentials on day 7. NK cells from *Mirc11*$^{-/-}$ mice were able to mediate cytotoxicity against B16F10 cells; however, the level was moderately reduced compared to the NK cells from WT mice. In comparison, cytotoxicity against any other target cells was comparable to that of NK cells from WT mice (Supplementary Figure 1B). Given this

outcome, we analyzed IL-15-cultured NK cells against these target cells. The cytotoxic potentials of IL-15-cultured NK cells from *Mirc11*$^{-/-}$ mice was moderately reduced against B16F10, EL4^{H60}, RMA/S, and YAC1 compared to NK cells from WT mice (Supplementary Figure 1C). To further validate these observations, we analyzed the degranulation capacity of NK cells using CD107a surface localization as a marker for the release of cytotoxic granules in co-culture experiments. Expression of CD107a by IL-2- or IL-15-cultured NK cells was consistent with the direct cytotoxicity (data not shown). These findings imply that the lack of *Mirc11* complex leads to a moderate reduction in the cytotoxic potentials of NK cells. IL-2, but not IL-15, helps NK cells from *Mirc11*$^{-/-}$ mice to overcome this defect. These findings are consistent with the role of IL-2, which is known to bypass the requirement of WASp-dependent actin polymerization in NK cells (57).

To further define the role of the *Mirc11* cluster in regulating NK cell-mediated *in vivo* cytotoxicity, we utilized a transplant rejection model. Host WT or *Mirc11*$^{-/-}$ (both H-2^{b}, H2-K^{b} & H2-D^{b}) mice were challenged with donor-derived splenocytes from C57BL/6 (H-2^{b}, H2-K^{b} & H2-D^{b}; '*self*'), β2m^{tm1Unc}/J (H-2^{b}; but, negative for cell surface H2-K^{b} & H2-D^{b}; '*missing-self*') and BALB/c (H-2^{d}, H2-K^{d} & H2-D^{d}; '*non-self*') mice. Donor splenocytes along with C57BL/6 splenocytes were labeled with cell-trace vital dyes. Labeled cells were mixed in a 1:1:1 ratio (C57BL/6-CFSE; β2m^{tm1Unc}/J-CFSE/CTV; and BALB/c-CFSE/CTR) and injected into either WT or *Mirc11*$^{-/-}$ mice. Eighteen hours later the host spleens were harvested and analyzed by flow cytometry for remaining vital-dye positive donor-derived splenocytes. The number of remaining donor splenocytes represented a surrogate marker for the level of NK cell-mediated killing. We observed that the loss of *Mirc11* significantly impaired the ability of NK cells to clear '*missing-self*' cells from β2m^{tm1Unc}/J mice; however, they were able to kill '*non-self*' BALB/c-derived donor splenocytes comparable to WT (Supplementary Figure 1D). Along with the data collected from co-culture experiments, these results suggest NK cells partially rely on *Mirc11* for regulation of cell-mediated cytotoxicity.

Mirc11 is essential for proinflammatory responses of NK cells

A second primary effector function of NK cells is to regulate both innate and adaptive immune cells via the production of pro-inflammatory cytokines, such as IFN-γ, GM-CSF, and various chemokines (58). To address whether the lack of *Mirc11* complex affects the production of inflammatory cytokines, IL-2- or IL-15-cultured NK cells were co-cultured with different tumor targets to determine the percentage of IFN-γ positive NK cells (Figure 1A & B). A lack of *Mirc11* complex significantly impaired the ability of NK cells to produce IFN-γ with all the tumor targets tested. Although culturing NK cells from *Mirc11*$^{-/-}$ mice with IL-2 helped to overcome the defect in mediating anti-tumor cytotoxicity, it did not rescue the defect in the production of IFN-γ (Figure 1A). To further dissect the specific signaling pathways that are affected by the absence of *Mirc11* complex, we stimulated NK cells with plate-bound mitogenic antibodies that target specific activation receptors. Splenic NK cells from WT and *Mirc11*$^{-/-}$ mice were cultured with IL-2 and activated with anti-NKG2D (DAP10 & DAP12), anti-NCR1 (Fc εRIγ and CD3ζ), anti-CD137 (Lck-Fyn and TRAF2), anti-CD244 (SAP-Fyn), or anti-Ly49H (DAP10 and DAP12) antibodies. Culture supernatants were collected and analyzed for IFN-γ, TNF-α, GM-CSF,

CCL3 (MIP1α), CCL4 (MIP1β), and CCL5 (RANTES). Generation of these cytokines and chemokines was significantly impaired in NK cells from *Mirc11*$^{-/-}$ mice compared to those from WT mice (Figure 1C). In addition to stimulation through germline-encoded activation receptors, IL-12 and IL-18 can induce NK cells to produce proinflammatory cytokines and chemokines (59). IL-12 receptor consists of IL-12Rα and IL-12Rβ and mediates signaling via a JAK2/STAT4-mediated pathway (60, 61). IL-18 receptor (IL-18Rα and IL-18Rβ) mediate signals via the MyD88/IRAKs/TRAF6 complex. Given these differences in activation- versus cytokine receptor-mediated signaling, we speculated that the *Mirc11* complex might not function to regulate IL-12 and IL-18-mediated activation of NK cells. Analyses of the culture supernatants revealed that production of IFN-γ, GM-CSF, CCL3, CCL4, and CCL5 was comparable between *Mirc11*$^{-/-}$ and WT. These results demonstrate that the function of Mirc11 is required for NK cell-mediated cytokine production downstream of activation receptor signaling, and that lack of the *Mirc11* complex did not render NK cells into a collective hyporesponsiveness.

To employ an unbiased approach to identify target genes regulated by the *Mirc11* cluster, we performed transcriptome-wide RNA sequencing analyses. Purified IL-2-cultured splenic NK cells were activated with plate-bound anti-NKG2D mAb (A10, 5 μg/ml); total mRNA was isolated, transcribed, and sequenced. Single-end reads of transcripts from a NextSeq500 that went through base-quality trimming were used. Unsupervised analyses of transcriptional profiles of non-stimulated and anti-NKG2D mAb-activated NK cells using principal-component analyses (PCA) revealed that stimulated NK cells from the WT mice possess a transcriptome that is distinct from that of NK cells from *Mirc11*$^{-/-}$ mice, as well as the unstimulated controls from either of the strains (Supplementary Figure 3A). Additionally, a low percent variance among three mice for each strain or condition clustered together in dispersion matrices indicated consistency among samples. We then used statistical filtering ($p < 0.05$ Mann–Whitney, Benjamini–Hochberg correction of stimulated versus non-stimulated) to identify clusters of genes that corresponded to different conditions based on similarity of available transcripts. Among the non-stimulated controls, a set of 255 genes was distinctly expressed in NK cells from the WT that were low or not expressed in the NK cells from *Mirc11*$^{-/-}$ mice (Figure 1D). Following anti-NKG2D mAb-mediated activation, NK cells from WT mice differentially expressed 1074 transcripts compared to the unstimulated NK cells, of which 240 overlapped between WT and *Mirc11*$^{-/-}$ mice. A total of 834 genes were uniquely expressed in NK cells from the WT following anti-NKG2D mAb-mediated activation, which was either significantly low or absent in the NK cells from *Mirc11*$^{-/-}$ mice. Given that the NK cells from *Mirc11*$^{-/-}$ mice developed normally yet lacked responsiveness to anti-NKG2D stimulation, we hypothesized that *Mirc11*$^{-/-}$ likely regulates the inflammatory response and effector function in activated mature NK cells. Indeed, comparison of the differentially expressed transcripts between the anti-NKG2D mAb stimulated WT, and *Mirc11*$^{-/-}$ NK cells revealed a dramatic attenuation of the expression of proinflammatory cytokines, chemokines, and cytotoxic granule-associated factors in the *Mirc11*$^{-/-}$ NK cells (Figure 1E, F). Collectively, these findings reveal that the *Mirc11* cluster plays a requisite role in positively regulating the production of multiple pro-inflammatory factors, which was consistent with our analyses of the supernatants from co-culture and plate-bound mitogenic antibody-mediated activations.

Mirc11 cluster is obligatory for NK cell-mediated *in vivo* clearance of *Listeria monocytogenes*.

IFN-γ produced by NK cells during the early phase of infection is crucial for the clearance of the facultative intracellular Gram-positive bacteria *Listeria monocytogenes* (62, 63). To evaluate the role of the *Mirc11* cluster in regulating proinflammatory cytokines, we systemically infected mice with 2×10^4 live *L. monocytogenes* (~0.5 LD_{50}). We tested the expressions of individual members of the *Mirc11* cluster in the purified splenic NK cells at 48 hours post-infection compared to NK cells from non-infected mice. Significant changes in the expression were observed for the *miR-27a* transcript followed by the *miR-24-2*, and the *miR-23a*, suggesting that a regulatory function of these transcripts is active during Listeria infection (Figure 2A). To determine the importance of the *Mirc11* cluster in the function of NK cells during Listeria infection, we analyzed the severity of the listeriosis by measuring the clearance of *L. monocytogenes* in the infected mice (64, 65). Compared to the WT mice, the number of bacteria in the livers of *Mirc11*$^{-/-}$ mice was persistently higher at 48 hours post-infection (Figure 2B). To determine if the increased bacterial load was associated with defects in NK cell function, we analyzed the percentages of IFN-γ-producing CD3ε$^-$NK1.1$^+$ NK cells in the spleens of the infected mice. We observed a significant reduction in the percentages of IFN-γ-positive CD3ε$^-$NK1.1$^+$ NK cells from *Mirc11*$^{-/-}$ compared to WT mice Figure 2C) during *L. monocytogenes* infection.

Because the *Mirc11*$^{-/-}$ mice are a global gene knockout model, to ensure that the impairment in cytokine production observed in *Mirc11* NK cells is intrinsic, we generated mixed bone marrow chimeras. Equal numbers of BM-derived cells from WT (CD45.1$^+$; B6.SJL) and *Mirc11*$^{-/-}$ (CD45.2$^+$; C57BL/6) mice were transferred into *Rag2*$^{-/-}\gamma_c^{-/-}$ double knockout mice. Six weeks later both groups were challenged with 2×10^4 *L. monocytogenes*. Forty-eight hours post-infection, spleens were analyzed for the percent IFN-γ-positive CD3ε$^-$NK1.1$^+$ NK cells. Whereas the percentage of NK cells did not differ indicating comparable levels of survival between the two genotypes (Figure 2D), the IFN-γ production was significantly reduced in NK cells from *Mirc11*$^{-/-}$ compared to that of WT mice (Figure 2E).

To further assess transcriptomic changes resulting from the loss of the *Mirc11* in NK cells, WT, and *Mirc11*$^{-/-}$ mice were challenged with 2×10^4 *L. monocytogenes*. Forty-eight hours later, CD3ε$^-$NK1.1$^+$ NK cells were sorted from the spleens of infected mice, and total mRNA from three mice for each group (unchallenged or challenged) were sequenced. Unsupervised analyses of transcriptomic profiles of unchallenged and *L. monocytogenes*-challenged mice using PCA revealed that NK cells from the WT mice demonstrated a transcriptome that is distinct from NK cells from *Mirc11*$^{-/-}$ mice (Supplementary Figure 3A). The consistency in transcript expression among samples was confirmed by the limited percent variance and the extent of their clustering on a dispersion matrix. Statistical filtering ($p < 0.05$ Mann–Whitney, Benjamini–Hochberg correction of stimulated versus non-stimulated) provided clusters of genes based on similarity of available transcripts. Subsequent statistical analyses revealed the differentially expressed genes in the WT and *Mirc11*$^{-/-}$ mice. NK cells derived from WT and *Mirc11*$^{-/-}$ mice challenged with *L. monocytogenes* showed a differential expression of 6519 and 7537 genes, respectively. NK

cells from the spleen of the non-challenged WT and *Mirc11*$^{-/-}$ mice had a differential expression of 3433 and 4184 genes, respectively. In NK cells derived from non-challenged mice, a set of 740 genes were differentially expressed in WT compared to that of *Mirc11*$^{-/-}$ mice with a difference in the expression of two- or more fold change in either direction. (Figure 2F). Following *L. monocytogenes*-challenge, NK cells from WT mice expressed 5302 transcripts, of which 1217 overlapped with the *Mirc11*$^{-/-}$ mice. After normalizing the level of each transcript in the NK cells from *Mirc11*$^{-/-}$ to the WT, we plotted all the genes using Volcano plots to determine the overall change in the transcriptomic profile (Figure 2G). The red dots represent genes that are significantly increased, while the dark blue dots represent genes that are significantly decreased in NK cells from *Mirc11*$^{-/-}$ mice compared to WT. Analyses of a select panel of transcripts encoding pro-inflammatory factors using heat maps of normalized expression values (Log_2) revealed the inability of NK cells from *Mirc11*$^{-/-}$ mice to transcribe many of these genes (Figure 2H). Consistent with our findings from *in vitro* NK cell activations and the intracellular staining of IFN-γ in NK cells derived from the spleens of the *L. monocytogenes* infected mice, transcripts that encode many proinflammatory cytokines (*Ifng*, *Lif*, *Tnfa*, *csf2*) chemokines (*Ccl22*, *Ccl19*, *Ccl17*, *Ccl8*, *Ccl12*, *Ccl7*), cytotoxic granules-associate factors (*Gzmc*, *Gzmb*, *Pfr1*, *Gzmf*, *Gzma*) and interleukins (*Il10*, *Il17a*, *Il27*, *Il6*, *Il12a*, *Il15*, *Il22*, *Il22b*, *Il18*, *Il23a*, *Il7*, *Il2*, *Il4*) were reduced by more than 50 percent in NK cells from the *Mirc11*$^{-/-}$ mice relative to the WT controls (Figure 2H). These findings reveal that the *Mirc11* cluster plays an essential role in positively regulating the production of multiple pro-inflammatory factors and specifically an alteration but not a reduction in the transcriptome argues that the lack of *Mirc11* did not lead to a global hyporesponsiveness of NK cells.

Mirc11 cluster is required for NK cell-mediated *in vivo* clearance of B16F10 melanoma

To evaluate the role of the *Mirc11* cluster in regulating anti-tumor response *in vivo*, we used a B16F10 melanoma-based pulmonary pseudometastases model (66), where the host mice depend on NK cell-mediated IFN-γ production for tumor clearance (67). We hypothesized that an impairment in the ability of *Mirc11*$^{-/-}$ NK cells to produce IFN-γ and other inflammatory cytokines could result in a failure to clear B16F10 tumor cells. WT and *Mirc11*$^{-/-}$ mice were challenged intravenously with two different doses of B16F10 cells (2×10^5 or 1×10^6). Fourteen days later, the lungs of the challenged mice were harvested, perfused, and the number of nodules was counted. Gross analyses and Hematoxylin & Eosin staining indicated a considerable number of pseudometastases in the lungs of *Mirc11*$^{-/-}$ mice compared to WT mice (Figure 2I). Quantification of nodules substantiated this observation, as lungs from the *Mirc11*$^{-/-}$ mice have a significantly higher number of nodules compared to the lungs from WT mice (Figure 2J). To correlate these functional impairments with an expression of *Mirc11* cluster members, we analyzed the relative amounts of *miR-23a*, *miR-27a*, and *miR-24-2*, 48 hours following B16F10 injection in WT mice. Expression of *miR-23a*, *miR-24-2*, and *miR-27a* increased following tumor challenge compared to that of non-challenged mice with *miR-23a* and *miR-27a* being dominant (Figure 2K). These data suggest an increase in the expression of the *Mirc11* cluster correlates with an augmented ability of NK cells to mediate clearance of B16F10 melanoma tumors.

Identification of target transcripts of the *Mirc11* cluster in NK cells

To define the molecular mechanism that causes the impairment in the production of protective pro-inflammatory factors during *L. monocytogenes* infections in the *Mirc11*$^{-/-}$ mice, we next identified the mRNA targets of the *Mirc11* cluster. The mature sequences of all three members of the *Mirc11* cluster were found in the NK cells from the WT mice during *L. monocytogenes* infection and anti-NKG2D mAb-mediated activation. Therefore, we speculated that the genetic ablation of the *Mirc11* cluster in NK cells would augment the half-life and relieve the translational repression of target mRNA transcripts and that identifying potential targets with differential expression in WT and *Mirc11* NK cells would define sources of NF-κB and AP-1 inhibition. Using transcriptome-wide RNA sequencing data, we determined the target transcripts that are differentially enriched using Fisher's exact test between splenic NK cells that were derived from the non-challenged and *L. monocytogenes*-challenged WT and *Mirc11*$^{-/-}$ mice. Potential targets of *miR-23a*, *miR-27a*, and *miR-24-2* were identified based on the presence of the unique 'seed' sequences present in the 3′ UTR of the transcripts (Figure 3A). Utilizing TargetScan 7.1-based *in silico* analyses (http://www.targetscan.org), we identified a set of target mRNAs that were present in the total genome-wide RNA sequence analyses of NK cells from WT and *Mirc11*$^{-/-}$ mice based on 'the aggregate probability of conserved targeting' (P_{CT}) (68). *In silico* predictions that matched the 3′ UTR of the transcripts and their orthologs based on the UCSC whole-genome alignments, identified a total of 6,606 genes that could be targeted by *Mirc11* cluster (Figure 3A). Among these 5,972 were present in the RNA sequencing data obtained from splenic NK cells following *L. monocytogenes* infection (Figure 3B). Only a fraction of them (617) were differentially expressed between WT and the *Mirc11*$^{-/-}$ mice under non-challenged condition (Figure 3C). However, following *Listeria* challenge 2073 of these transcripts were differentially expressed between the NK cells derived from WT and the *Mirc11*$^{-/-}$ mice (Figure 3D). Among the three, lack of *miR-24-2* was associated with the most differentially expressed genes (1169) followed by *miR-23a* (1145) and *miR-27a* (394). A considerable number of these transcripts can be targeted by one or more of the three miRNAs.

Analyses of the identities of the transcripts altered by *miRNA-23a*, *miRNA-24-2*, and *miRNA27a* revealed that they fall into multiple categories including genes that control apoptosis and cell survival, metabolic regulators, transcriptional activators of cytokines and chemokines, and signaling proteins (Figure 3E, F, & G). The first group is the transcripts-encoding transcriptional activators (*Stat1, Ctnnb1p1, Zfp799, Zfp113, Zfp397, Zfp329, IRF4, Pparg*) or repressors (*ATF3, Runx2, Hic2*) that may have direct control over the production of inflammatory cytokines and chemokines. Alterations in the transcript levels of ATF3, IRF4, and Runx2 may provide potential mechanisms. We find the transcript levels of ATF3 reduced in NK cells from *Mirc11*$^{-/-}$ mice compared to that of WT. Earlier work has described the ATF3 interacts with the *cis*-regulatory element and repress the transcription *Ifng* gene (69). Thus, the reduction in ATF3 does not correspond to the reduction in IFN-γ or other inflammatory cytokine production that we observe in *Mirc11*$^{-/-}$ mice. Following *L. monocytogenes* infection, we observed a modest increase in IRF4-encoding transcripts in the NK cells from the WT but not in *Mirc11*$^{-/-}$ mice. In terms of the transcriptional activators, it is possible changes in the activity of one of these factors could lead to differential expression

of several cytokines or chemokines. However, the fact that genes beyond the actual cytokines and chemokines were altered suggests the regulatory function of *Mirc11* acts on targets with a broader transcriptional network. For example, IRF4 cooperates with basic leucine zipper transcription factor ATF-like (BATF)-Jun heterodimers and initiates transcription by binding to AP-1-IRF4 composite elements (AICE) (70, 71). This suggests a reduction in *Irf4* transcript would not induce the hypo-inflammatory response observed in NK cells from *Mirc11*$^{-/-}$ mice in response to stimulation via activation receptors. Similarly, Runx2 can function both as a repressor and a transactivator of select genes in multiple cells types (72, 73). Runx2 was considerably reduced in NK cells from WT compared to *Mirc11*$^{-/-}$ mice that were infected with *L. monocytogenes*. Like IRF4, however, the specificity of the transcriptional network regulated by Runx2 suggests this alteration is insufficient to explain the functional defects of NK cells in *Mirc11*$^{-/-}$ mice.

Based on this line of thinking, we hypothesized that altered activity of a membrane proximal signaling protein immediately downstream of activation receptors could lead to the broader changes in transcription seen in the *Mirc11*$^{-/-}$ NK cells. Thus, we decided to focus our analysis on the group of potential targets that included components of activation receptor signaling. This group included both mediators (Itpk1, Mtss1, PLC-H1, Rictor) and repressors (A20/Tnfaip3, Fbxl17, RNF170, Cbl-b) of activation receptor signaling. Interestingly, the ubiquitin regulators (A20/Tnfaip3, Fbxl17, RNF170, Cbl-b) target multiple substrates including membrane proximal TRAF6, TRAF2, RIPK1, RIPK2, and TAK1, which function as central signal transducing modules downstream of TCR (74) and BCR (75) in the activation and nuclear translocation of NF-κB and AP-1. Thus, alterations in the translational threshold of ubiquitin modifiers provided the most plausible mechanism for the hypo-inflammatory responses of NK cells of the *Mirc11*$^{-/-}$ mice.

Mirc11 cluster targets NF-κB and AP-1-mediated gene transcription

Transcriptional induction of proinflammatory factors is primarily mediated by the activation of two major transcription factor complexes NF-κB (p50/RelA) and AP-1 (c-Fos/c-Jun) (76). Analyses of the activation status of Jnk1/2 that is upstream of NF-κB and AP-1 revealed a considerable reduction in their phosphorylation following anti-NKG2D mAb-mediated activation (Supplementary Figure 3B). Similar reductions were seen in the phosphorylation of Erk1/2; but not p38. Because we observed global defects in inflammatory factor production in NK cells from *Mirc11*$^{-/-}$ mice, we hypothesized activation of one or both the primary transcriptional networks was disrupted by a lack of the *Mirc11* cluster. To define the effect of the *Mirc11* cluster on NF-κB and AP-1 activation, we performed *in silico* regulatory network genome-wide analyses using DeMAND (77) and a precompiled Bayesian network based on the gene expression profiles of 254 B cell lymphoma cell preparations on U95av2 arrays. Following stimulation with anti-NKG2D mAb, the DeMAND analysis revealed that the Rel-A (p65, $P < 10^{-7}$) and Jun ($P < 10^{-8}$) networks were significantly altered between the WT and *Mirc11*$^{-/-}$ NK cells (Supplementary Figure 4A & B). Likewise, gene network analysis using the IPA software tool revealed that the NF-κB ($p < 10^{-42}$) and AP-1 ($p < 10^{-13}$) pathways were significantly enriched among the differentially expressed gene-sets in NK cells derived from the *L. monocytogenes*-challenged WT and *Mirc11*$^{-/-}$ mice (Figure 4). A total of 280 differentially

expressed genes were identified with 64 were upregulated, and 216 downregulated that are transcriptionally regulated by NF-κB. A total of 320 differentially expressed genes were identified with 132 were upregulated and 188 downregulated that are the target genes of AP-1 complexes. Hierarchical clustering revealed multiple distinct gene groups either up- or downregulated as presented in heat maps (Figure 4A & B). Functional classification and Fisher's exact test further identified enriched transcripts that encode pro-inflammatory cytokines, chemokines, and other transcription factors. Collectively, these data further support that the altered response of NK cells from *Mirc11*$^{-/-}$ mice compare WT mice is most likely due to disruption of key transcriptional mediators of inflammatory response, such as NF-κB and AP-1.

To validate these *in silico* findings, we determined the functional status of both NF-κB and AP-1 in NK cells from *Mirc11*$^{-/-}$ mice. To do this, we stimulated NK cells derived from the WT and *Mirc11*$^{-/-}$ mice with plate-bound anti-NKG2D mAb, prepared nuclear lysates, and quantified the levels of binding of NF-κB and AP-1 to chromosomal DNA using electrophoretic mobility shift assay (EMSA). Gel-shift assays demonstrated that both NF-κB and AP-1 pathways are activated in NK cells derived from WT mice; however, are considerably reduced in NK cells from *Mirc11*$^{-/-}$ mice (Figure 5A).

Next, we combined the gene expression profiles (GEP) from both the RNA-seq libraries made from NK cells following anti-NKG2D mAb-mediated activation and from the *ex vivo* isolated fresh splenic NK cells from *L. monocytogenes* infected mice to identify shared and common targets. NK cells from *L. monocytogenes* challenged mice (WT versus *Mirc11*$^{-/-}$ mice) contained the 6073 genes that were differentially expressed compared to 628 genes that were differentially expressed in NK cells that were stimulated *in vitro* with anti-NKG2D mAb (WT versus *Mirc11*$^{-/-}$ mice). There were 446 genes that were shared between the two RNA-seq libraries, of which many were known to be transcriptionally regulated by NF-κB, AP-1, or both (Figure 5B). These shared group of genes included proinflammatory cytokines and chemokines. Genes that are regulated by NF-κB or AP-1 were visualized with Log_2–fold-change scatter plot. Expression of most of the target genes in NK cells from *Mirc11*$^{-/-}$ mice was significantly reduced, indicating that the *Mirc11* cluster functions as a central repressor of one or more negative regulators of NF-κB and AP-1 activation pathways (Figure 5C). Also, we evaluated the gene set enrichment for NF-κB and TNF-α response pathways. Analysis of NK cells stimulated either *in vitro* with anti-NKG2D mAb or derived from *L. monocytogenes* infected mice revealed these pathways were significantly impaired in NK cells lacking the *Mirc11* cluster (FDR adjusted $p < 0.05$) that was stimulated either *in vitro* with anti-NKG2D mAb or derived from *L. monocytogenes* infected mice (Figure 5D). Overall, transcriptome-wide RNA sequencing analyses revealed that the primary target genes of the *Mirc11* cluster involved transcriptional regulation by NF-κB and AP-1 complexes. Importantly, NK cells from WT mice infected with *L. monocytogenes* exhibited proinflammatory gene-set similar to that of human chronic inflammatory bowel disease; however, NK cells from *Mirc11*$^{-/-}$ mice lacked this differentially-expressed gene simulation (Supplementary Figure 5). This correlation supports the notion that *Mirc11* cluster optimizes pro-inflammatory responses.

A20, Cbl-b, and Itch are direct targets of the *Mirc11* cistron in mice and human

Given the significant reduction in the expression of genes that are transcriptionally regulated by the canonical NF-κB (RelA) and AP-1 (c-Fos/c-Jun) pathways, we hypothesized that deubiquitinating enzymes and E3 ligases with membrane proximal functions could be one of the principal targets of the *Mirc11* cluster. We analyzed two deubiquitinating enzymes (A20 and Cyld) and two E3 ligases (Cbl-b and Itch) with established roles in NF-κB and AP-1 signaling (78) in *ex vivo* purified splenic NK cells 48 hours after *L. monocytogenes* infection. NK cells from non-infected WT mice contained all four proteins (Figure 6A). Upon *L. monocytogenes* infection splenic NK cells from WT mice considerably reduced the expression of Cbl-b, Cyld, and Itch, while the levels of A20 remained undetectable. Additionally, NK cells from *Mirc11*$^{-/-}$ mice contained significantly augmented levels of A20, Cbl-b, Cyld, and Itch regardless of the infection status. We next validated these results in IL-2-cultured splenic NK cells that were activated with plate-bound anti-NKG2D mAb for varied periods of time. NK cells from WT mice contained all four proteins; however, NK cells from *Mirc11*$^{-/-}$ mice contained significantly increased levels of A20, Cbl-b, Cyld, and Itch (Figure 6B). Though activation with anti-NKG2D mAb increased the protein levels of A20, Cbl-b, Cyld, and Itch in NK cells from both WT and *Mirc11*$^{-/-}$ mice, NK cells from *Mirc11*$^{-/-}$ mice contained significantly a higher amount of A20, Cbl-b, Cyld, and Itch under both conditions. Our data suggest these regulatory proteins suppress *Mirc11*$^{-/-}$ NK cells due to a lack of microRNA mediated-silencing.

To identify the mechanistic link between the *Mirc11* cluster and these E3 ligases, we analyzed the 3′ UTR sequences of A20, Cbl-b, Cyld, and Itch. Using TargetScan (http://www.targetscan.org), we found that the 3′ UTR of all four E3 ligases contained predicted binding sites for one or more members of the *Mirc11* cluster (Figure 6C). To identify whether *miRNA23a*, *miRNA24-2*, or *miRNA27a* could directly target *Tnfaip3* (A20), *Cblb*, *Cyld*, and *Itch* mRNAs, we cloned their putative interacting sequences from 3′ UTR regions downstream of the firefly *luciferase* reporter gene in a pMIR-Report vector. We identified and cloned one, two, three, and two 3′ UTR regions of *Tnfaip3*, *Cblb*, *Cyld*, and *Itch*, respectively (Figure 6C). Control mimetics (CM) were cloned into a pMIR-Report vector used to quantify the background luciferase activity. These cloned sequence-containing pMIR-Report vectors were co-transduced with vectors expressing *miRNA23a*, *miRNA24-2*, *miRNA27a*, or control mimetics-encoding vectors into HEK293T cells. After 48 hours, cells were lysed, and the luciferase activity was quantified. The 3′ UTR of *Cblb* contained two seed matches between 3216–3236 and 5879–5901 nts targeted by *miR-27a*-3p and *miR-23a*-3p, respectively. Although the proximal seed match sequence for *miR-27a*-3p contained 13 non-contiguous nucleotides (out of 21) that were complementary, it was unable to block the translation of luciferase. However, the distal sequence that was targeted by *miR-23a*-3p with a 7mer seed match was functional as indicated by the reduction in luciferase activity. The 3′ UTR of *Cyld* contained three sequences between 3842–3864, 4031–4051, and 5979–6000 nts, which all targeted by *miR-24-2*-3p. Irrespective of the presence of three optimal seed matches, none of these were able to block the translation of luciferase. In this context, it is important to note that *miR-24–1*, the paralog of *miR-24-2*, contains an identical sequence (79). The 3′ UTR of *Itch* contained two seed matches between 2882–2900 and 4649–4669 nts that were targeted by *miR-27a*-3p and *miR-23a*-3p,

respectively. Incorporation of the target sequences in the 3′UTR of luciferase indicated that the *miR-27a*-3p was able to reduce the translation of luciferase but not the *miR-23a*-3p. Collectively, we found *miRNA23a* significantly reduced the luciferase activity of vector that contained the 3′ UTR of *Tnfaip3*. Similarly, *miRNA27a* reduced luciferase activity of vectors containing 3′ UTR sequences of either *Cblb* or *Itch* (Figure 6D). With three different 3′ UTR sequences of *Cyld*, we did not observe any reduction of luciferase activity indicating that *Mirc11* cluster members may not target Cyld (Figure 6D). Together, these data suggest the *Mirc11* cluster controls the activity of A20, Cbl-b, and Itch in NK cells by binding to the 3′ UTR of their respective transcripts and regulating their translation.

We next determined if this regulatory mechanism was also active in human NK cells. We purified $CD3e^{-}CD56^{+}$ NK cells from human peripheral blood mononuclear cells (PBMC) and transduced them with lentiviral pLenti-TetCMV vectors encoding individual pre-miRs or all three pre-miRs that encode the members of the *Mirc11* cluster. NK cells were activated with plate-bound anti-NKG2D mAb (1D11, 5 μg/ml)) for 24 hours and the percent IFN-γ-positive cells was quantified by flow cytometry. Our data show transduction of pre-*miR23a* or pre-*miR-27a* increased the percent IFN-γ^{+} NK cells compared to that of empty vector (Figure 6E). Out of four individual PBMCs transduced with pre-*miR24-2*, only one showed an augmentation of percent IFN-γ^{+} NK cells. Collectively, these results indicate the *Mirc11* cluster reduces the protein translation of specific deubiquitinating enzymes or E3 ligases to allow maximum threshold of signaling strength downstream of activation receptors such as NKG2D.

Mirc11-mediated targeting of A20, Cbl-b, and Itch augments K63-polyubiquitination of TRAF6

NKG2D-mediated activation rapidly stimulates p50/RelA (NF-κB) and c-Fos/c-Jun (AP-1) activation and nuclear translocation (25). TRAF6 and TRAF2 are effector E3 ligases that synthesize lysine (K) 63-linked ubiquitin chains on themselves and other substrates resulting in their activation (80). Deubiquitinating enzymes A20 or Cyld and E3 ligases Cbl-b or Itch limit this activation by removing non-degradative K63-polyubiquitination of TRAF6 and TRFA2 (81). In addition to removing this activating post-translational modification, A20 functions as a ubiquitin-editing enzyme by removing K63-polyubiquitination and adding K48-polyubiquitination to its substrates marking them for proteasomal degradation (82). Therefore, to establish the roles of A20, Cbl-b, Cyld, and Itch as suppressors of NK cell activation, we used their respective gene knockout mice. We first analyzed the maturation and development of NK cells in these mice. A total number of NK cells among the splenic lymphocytes between the knockout mice to their respective WT controls were comparable, indicating that the lack of these proteins does not alter their lineage commitment and development (Supplementary Figure 6A). Terminal maturation of NK cells was analyzed by quantifying the expression of KLRG1 and CD27/CD11b ratio. Except for a moderate reduction in NK cells from $Cyld^{-/-}$ mice, the expression of KLRG1 was intact in all the knockout mice, demonstrating that the terminal maturation of NK cells is not altered (Supplementary Figure 6B). Similarly, the ratio of $CD27^{+}$, $CD27^{+}/CD11b^{+}$, $CD11b^{+}$ NK subsets were comparable between the knockout mice and their respective WT controls, demonstrating that their functional maturation is intact (data not are shown). Next, we tested

the NK cells from the various knockout mice for their anti-tumor cytotoxic potentials and the ability to produce proinflammatory cytokines. Splenic NK cells from *Tnfaip3*$^{fl/fl}$*Rosa*$^{Cre\text{-}ER}$ mice were cultured with IL-15 for seven days, and on day four tamoxifen was added to the culture to induce the deletion of A20-encoding alleles. Splenic NK cells from mice lacking *Cblb*, *Cyld*, and *Itch* were also prepared by culturing with IL-15. While NK cells from three of the knockout models mediated comparable levels of cytotoxicity against EL4^{H60}, RMA/S, and YAC1 compared to WT controls (Supplementary Figure 6C), NK cells that lacked Cbl-b exhibited an increased killing of EL4^{H60}, RMA/S, and YAC1. Next, we stimulated the IL-15-cultured NK cells with plate-bound anti-NKG2D mAb for 18 hours, and the supernatants were collected and analyzed for IFN-γ, GM-CSF, CCL3, CCL4, and CCL5 (Supplementary Figure 7). The absence of *Tnfaip3*, *Cblb*, *Cyld*, or *Itch* significantly increased the generation of these cytokines and chemokines; thus, corroborating data from the *Mirc11*$^{-/-}$ mice suggesting this regulatory mechanism primarily affects the production of proinflammatory factors. Together, these data demonstrate that A20, Cbl-b, Cyld, and Itch regulate proinflammatory responses of NK cells through their well-defined role in repressing the activation of NF-κB and AP-1.

A lack of *Mirc11* reduces K63- and increases K48-polyubiquitination of TRAF6

Long chain K63-polyubiquitination synthesized by the E3 ligase TRAF6 facilitates the recruitment of TAB2 and TAB3 to activate TAK1 (82). In turn, TAK1 phosphorylates and activate NF-κB-inhibitor kinases (IKKα and IKKβ) and eventual activation of the NF-κB complex (83). A20 contains both deubiquitinase and E3 ligase domains and functions as a ubiquitin-editing enzyme (84). A20 and Cyld can form independent complexes with Itch to disassemble K63 chains and to add K48 polyubiquitination (36, 85). Therefore, to confirm the specific mechanism by which these negative regulators function to suppress NK cell activation in the absence of *Mirc11*-mediated silencing, we next analyzed TRAF6 ubiquitination in NK cells from WT and *Mirc11*$^{-/-}$ mice following anti-NKG2D mAb-mediated activation. TRAF6 was immunoprecipitated from NK cell lysates and probed for K63 and K48 ubiquitination. We observed a ladder of high-molecular-mass of K63-polyubiquitinated TRAF6 in NK cells from the WT mice (Figure 7A, **lanes 1&2**). However, a diffused ladder of K63-polyubiquitinated TRAF6 was absent in NK cells from *Mirc11*$^{-/-}$ mice (Figure 7A, **lanes 3&4**). Next, we analyzed the immunoprecipitated TRAF6 for K48 polyubiquitination. At 15 minutes following anti-NKG2D mAb-mediated activation, TRAF6 in NK cells from the WT mice did not contain any K48 polyubiquitination (Figure 7B, **lanes 1&2**). In contrast, TRAF6 in NK cells from the *Mirc11*$^{-/-}$ mice contained considerable levels of K48 polyubiquitination (Figure 7B, **lanes 3&4**). Similarly, K63 ubiquitination of RIP1 was considerably augmented in NK cells from the WT mice, which was absent in NK cells from the *Mirc11*$^{-/-}$ mice (Figure 7C). We further validated TRAF2 following activation and did not observe any change in K63 (Figure 7D, **lanes 1–4**) or K48 (data not shown) ubiquitination, suggesting TRAF6 is the primary target of A20, Cyld, Cbl-b, and Itch-mediated suppression of NK cell-mediated cytokine production

To validate these findings, we incubated IL-15-cultured NK cells from WT and *Mirc11*$^{-/-}$ mice with mutant K63 or mutant K48 ubiquitin proteins. These recombinant ubiquitin proteins are mutated from lysine to arginine at K63 (K63R) and K48 (K48R), respectively

(86). These mutated ubiquitins can form an active thioester at the C-terminus and can be transferred to substrate proteins; however, they will not be able to form polyubiquitin chains with other ubiquitin molecules. Passive diffusion of these modified ubiquitins into NK cells bind to substrates and limit the ubiquitylation to mono-ubiquitination (86). We co-incubated NK cells with either K63R or K48R ubiquitins, activated with anti-NKG2D mAb, collected the supernatants and quantified the amount of IFN-γ. Incubation of NK cells from WT but not *Mirc11*$^{-/-}$ mice with K63R significantly reduced the production of IFN-γ, TNF-α, GM-CSF, CCL4, and CCL5 (Figure 7E). Addition of K48R to NK cells from neither WT nor *Mirc11*$^{-/-}$ mice augmented the production of these cytokines and chemokines. Based on these results, we conclude that *Mirc11* cluster temporally targets and silence these E3 ligases during the active-phase of receptor-mediated stimulation to enable optimal NK cell-mediated production of proinflammatory factors.

Discussion

Production of inflammatory cytokines and chemokines is a critical component of an immune response. However, an acute or a chronic inflammatory response is highly destructive; therefore, the tight regulation of genes that encode inflammatory factors is essential. In this study, we define the *Mirc11* cluster as an essential positive regulator of inflammatory cytokine and chemokine production. We demonstrate that one of the primary functions of the *Mirc11* cistron is to target and silence the translation of A20, Cbl-b, Cyld, and Itch. Lack of the *Mirc11* cluster led to the increased translation of A20, Cbl-b, Cyld, and Itch, which resulted in increased deubiquitylation of K63 and augmented K48 ubiquitylation of TRAF6. Degradation of TRAF6 dampen the activation and nuclear translocation of NF-κB and AP-1 complexes and therefore the transcription of pro-inflammatory genes. These findings provide insights into a novel immune regulatory function of miRNAs.

More than 400 and 300 miRNAs have been identified in human and mouse NK cells, respectively (87, 88). The *Mirc11* cistron encodes three independent miRNAs, *miR-23a*, *miR-24-2*, and *miR-27a* on mouse chromosome #8 (#19 in human) (89). *Mirc22* is a paralog of *Mirc11*, which encodes *miR-23b*, *miR-24–1*, and *miR-27b* located in mouse chromosome #13 (#9 in human) (79). Paralogs of miR-23 and miR-27 differ in one nucleotide, whereas the mature miR-24–1 and miR-24-2 are identical. Members of *Mirc11* (*miR-23a*, *miR-24-2*) and *Mirc22* (*miR-23b*, *miR-24–1*) clusters are expressed at a low but detectable levels compared to abundantly expressed *miR-150*, *miR-29a*, *miR-16*, *miR-21*, *let-7a*, *let-7f*, *miR-24*, *miR-15b*, *miR-720*, *let-7g*, *miR-103*, and *miR-26a* in mouse and human NK cells (90, 91). Earlier studies have shown miRNAs including *miR-181* (92), *miR-150* (93, 94), and *miR-15/16* (95) regulate the development and maturation of mouse or human NK cells. Lack of *miR-181* in *in vitro* human CD34^{+} HSC cultures (92) or in the *in vivo* absence of either *miR-150* or *miR-15/16* in mouse (93) significantly reduced the maturation and number of NK cells. However, lack of the *Mirc11* cluster did not alter the development, maturation, or trafficking of NK cells. BM, spleen, lung, liver, and peripheral blood of *Mirc11*$^{-/-}$ mice contained comparable numbers of mature NK cells compared to WT. Expression of activation (NKG2D, NCR1, CD244, Ly49D, Ly49H, and NK1.1) or inhibitory (NKG2A, Ly49A, Ly49C/I, Ly49G2) receptors was comparable between NK cells derived from *Mirc11*$^{-/-}$ and WT mice. Functional phenotyping using CD27, CD11b, and KLRG1

markers implied that the maturation of NK cells proceeds normally in the absence of *Mirc11*. Compared to *miR-181* that targets the mRNA encoding Nemo-like kinase (NLK), an inhibitor of Notch signaling (96); or *miR-150* and *miR-15/16*, which both target the mRNA encoding c-Myb (93, 95) a positive regulator of Myc and Bcl2, *Mirc11* does not appear to silence transcripts whose products are obligatory for the commitment, survival, and maturation of developing NK cells. One reason could be that although the members of the *Mirc11* cluster are present in naïve NK cells, their expression levels are comparatively low and are increased following activation of the NK cells either *in vitro* with plate-bound anti-NKG2D mAb or *in vivo* with *L. monocytogenes*. Data collected from this study suggests the *Mirc11* cluster has a novel role regulating NK cell-mediated cytokine production independent of a function in controlling NK cell lineage commitment and development seen in other miRNAs.

Lack of *Mirc11* cluster only moderately impaired the cytotoxic potentials of naïve or IL-15-cultured NK cells against $EL4^{H60}$, RMA/S, B16F10, and YAC1 targets. Culturing NK cells from $Mirc11^{-/-}$ mice with IL-2 fully rescued the impairment in their cytotoxicity. Analyses of the *in vivo* clearance of donor-derived splenocytes that either expressed significantly reduced levels of MHC Class I ($H\text{-}2^{b}$; β−2 microglobulin knockout C57BL/6 mice representing '*missing-self*') or a mismatched MHC Class I ($H\text{-}2^{d}$; BALB/c mice representing '*non-self*') revealed that the lack of Mirc11 impaired only the clearance of splenocytes representing '*missing-self*' and not '*non-self*'. Earlier studies have shown that one of the members of *Mirc11* cistron, *miR-27a* targets transcripts encoding Perforin and Granzyme B and the absence of *miR-27a* significantly augmented the cytotoxic potentials of human NK cells (97). Our transcriptomic profiling of NK cells from either *in vitro* anti-NKG2D mAb-stimulated or from *L. monocytogenes*-challenged mice revealed reductions in the expression levels of Perforin, Granzyme B, Granzyme A, Granzyme C, and Granzyme F in NK cells from $Mirc11^{-/-}$ mice. Irrespective of these observations; we observed neither a significant reduction nor an augmentation of NK cell-mediated cytotoxicity in co-culture experiments using the EL4-H60 model in which NK cells are activated specifically through NKG2D. This suggests the reduced expression of perforin and various granzymes is not sufficient to induce the differences in cytotoxicity seen in some of the models tested, and that another aspect of NK cell function is also disrupted. We hypothesized that impairments in other effector functions such as the production of proinflammatory cytokines might account for the reduction in cytotoxicity. NK cell-derived IFN-γ is known to augment both activating (ICAM1) and inhibitory (MHC Class I) ligands on target cells (98). Also, one of the mechanisms that NK cells utilize to recognize target cells via '*missing-self*' mechanism is to employ LFA-1 to interact with ICAM1 on target cells (99). Thus, a significant reduction in the production of IFN-γ by the NK cells from $Mirc11^{-/-}$ mice could exclusively affect the lysis of splenocytes from β−2 microglobulin knockout mice. Splenocytes from BALB/c mice express allo MHC Class I ($H2\text{-}K^{d}$ and $H2\text{-}D^{d}$) and H60, Rae-1, and MULT1 that are the ligands of the NKG2D receptor (100–102). This could explain why the recognition and the *in vivo* clearance of BALB/c-derived splenocytes is not impaired in $Mirc11^{-/-}$ mice.

To identify whether the production of IFN-γ is impaired in NK cells derived from $Mirc11^{-/-}$ mice, we co-cultured NK cells with EL4, $EL4^{H60}$, RMA, RMA/S, YAC1, and B16F10. Levels of IFN-γ were significantly reduced in the supernatants of NK cells from $Mirc11^{-/-}$

compared to those from WT mice in the co-culture models irrespective of the mechanism of target cell recognition. This revealed the inherent ability of NK cells to produce IFN-γ in the absence of *Mirc11* cluster is severely compromised. Unlike cytotoxicity, the defects in IFN-γ could not be rescued by culturing naïve *Mirc11*$^{-/-}$ NK cells either with IL-2 or IL-15. This indicated that the impairment in cytokine production is due a distinct alteration in the posttranscriptional mechanism that is regulated by the *Mirc11* cluster. Activation of IL-2-cultured NK cells from *Mirc11*$^{-/-}$ mice with plate-bound anti-NKG2D mAb further demonstrated a severe defect in the production of multiple proinflammatory cytokines (IFN-γ, GM-CSF) and chemokines (CCL3, CCL4, CCL5). This positive correlation of *Mirc11* and the generation of inflammatory cytokines is corroborated by data collected in T cells by showing that the enforced overexpression of the individual members or the full-cluster of *Mirc11* significantly elevated the production of IFN-γ, activation status (CD44^{Hi}CD62L^{Lo}), and cell proliferation in transgenic mice (47). In addition, this overexpression of *Mirc11* cluster resulted in the hyperactivation of T cells and differentially skewed the commitment of Th1, Th2, Th17, and induced T regulatory cells in a cytokine-dependent manner (47). An earlier study also shows that both *Mirc11* and *Mirc22* were involved in containing a Th2-mediated type-2 inflammation and lung pathology in an experimental mouse model of asthma (48). The mechanism was primarily attributed to an IL-4-based network that is regulated by transcription factors Ikaros1 and Gata3 (48). In another study, exposure of CD8^{+} T cells to tumor-derived TGF-β augmented the expression of the *Mirc11* cluster, which directly repressed the translation of BLIMP-1 (103). These data demonstrate the regulatory role of *Mirc11* extends beyond direct regulation of specific cytokines and chemokines and rather is required for maintaining a level of activation that enables generation of multiple proinflammatory factors. Along these lines, our genome-wide transcriptomic analyses of anti-NKG2D mAb stimulated *Mirc11*$^{-/-}$ NK cells further validate this role by demonstrating loss of *Mirc11*$^{-/-}$ induces a broad inability to generate multiple inflammatory factors as opposed to regulating individual cytokines and chemokines.

To further validate these *in vitro* findings and to define the role of the *Mirc11* cluster *in vivo*, we challenged WT and *Mirc11*$^{-/-}$ mice with *L. monocytogenes*, whose clearance depends on IFN-γ produced by NK cells early during infection (104). The absence of the *Mirc11* cluster impaired the clearance of *L. monocytogenes* and considerably reduced the number of NK cells that produced IFN-γ. Recent studies have shown that two members of the *Mirc11* cluster, *miR-23a*, and *miR-27a*, negatively regulate the expression of mitochondrial Peptidyl-prolyl cis-trans isomerase (PPIF) in T cells during an established (14 days) *L. monocytogenes* infection (105). By containing the expression levels of PPIF, *miR-23a* and *miR-27a* helped to maintain the mitochondrial integrity via restricting the influx of reactive oxygen species. This earlier study showed that the T cells lacking *miR-23a* and *miR-27a* were highly susceptible to TCR-mediated activation-induced cell death. Based on these data we may expect *Mirc11*$^{-/-}$ NK cells to exhibit increased cell death during Listeria infection. In contrast to these earlier studies, we neither observed an increase in the transcript levels of *Ppif* nor augmented cell death of NK cells during *L. monocytogenes* infections. We attribute two reasons for these differences. First, our study utilized the mice that lacked the entire *Mirc11* cluster. Secondly, NK cells mediate their effector functions during the early phase of Listeria infection (48 hours) and do not require a period of clonal expansion to mediate

effector functions. Differences in the magnitude of proliferation induced by NK cell activation receptors as opposed to TCR stimulation could lead to different metabolic requirements between NK cells and T cells during Listeria infection, thus leading to different requirements of the *Mirc11*-mediated mitochondrial regulation. Additional work is warranted to compare the differential roles of the members of the *Mirc11* cluster between NK and T cells.

NK cells can be primed by a number of interleukins, including IL-12, IL-15, IL-18, IL-27, and IL-35 that are primarily produced by dendritic cells (DCs) (106). This complex interplay between DCs and NK cells is critical for NK cell-mediated effector functions (107). Likewise, the trans-presentation of IL-15 by IL-15Rα from the cell surface of DCs to IL-15Rα/IL-2Rβ/IL-2Rγ complex on NK cells regulate NK cell development, proliferation and gene transcriptions (108, 109). Because our *Mirc11*$^{-/-}$ model is a global knockout model, it is possible a lack of Mirc11-mediated regulation of other immune cells, such as DCs, could cause the defect in NK cell-mediated cytokine production. Therefore, to differentiate the cell-intrinsic and -extrinsic effects of the *Mirc11* cluster in NK cells, we generated BM chimeras of WT (CD45.1^{+}; B6.SJL) and *Mirc11*$^{-/-}$ (CD45.2^{+}; C57BL/6) mice in *Rag2*$^{-/-}\gamma_c^{-/-}$ mice. A comparable number of WT (CD45.1^{+}) and *Mirc11*$^{-/-}$ (CD45.2^{+}) CD3ε^{-}NK1.1^{+} NK cells in the spleens of *Rag2*$^{-/-}\gamma_c^{-/-}$ mice further confirmed a negligible role of the *Mirc11* cluster in the development and maturation of NK cells. We then infected the chimeric mice with listeria and evaluation of the NK cells *ex vivo* revealed the *Mirc11*-sufficient host did not rescue the defect in the production of IFN-γ, implying a cell-intrinsic role of *Mirc11* in NK cells. The absence of the *Mirc11* cistron significantly reduced the overall level of NK cell activation (5302 versus 740 differentially expressed transcripts with 1217 shared transcripts) following *L. monocytogenes* challenge, indicating activation receptor proximal regulation. Utilization of a pulmonary pseudometastasis model further confirmed the relationship between the *Mirc11* cluster and production of IFN-γ, which is obligatory for the clearance of B16F10. Importantly, augmentation of the expressions of *miR-23a*, *miR-24-2*, and *miR-27a* in NK cells *in vivo* during *L. monocytogenes* and B16F10 challenge demonstrates a requirement of *Mirc11* cluster-mediated function over a broad range of pathological conditions.

Uncontrolled inflammation forms the basis for allergy, asthma, and multiple autoimmune disorders (110). Myriad signaling pathways have been implicated in initiating inflammatory responses. Among these, the NF-κB/Rel and AP-1 families of transcription factors play an indispensable role in the transcription of genes encoding inflammatory factors (111). Transcriptomic signature of NK cells that lack *Mirc11* either obtained following anti-NKG2D-mediated activation or from *in vivo L. monocytogenes* infection strongly predicted defects in the activation of NF-κB/Rel, AP-1, or both. A considerable decrease in the nuclear translocations of the NF-κB/Rel and AP-1 in NK cells lacking *Mirc11* corroborates the significant reduction in the transcript levels of genes that are positively regulated by these transcription factors. Reduction in the transcripts encoding *Myc*, *Irf4*, *Jun*, *Nfkbia*, *Cd69*, *Il2ra*, *Atf3*, and *Cd83* in NK cells from *Mirc11*$^{-/-}$ mice demonstrates a complete failure of NF-κB/Rel-mediated transcriptional regulation. Similarly, a considerable reduction in the transcript levels of *Atf4*, *Ccnd2*, *Dusp3*, *Nfe2l1*, *Stk40*, and *Ztbt32* that are direct targets of AP-1 confirmed a significant reduction in its transcriptional activity. These

findings demonstrate that the *Mirc11* cluster is an active repressor of signaling pathways that inhibit the activation and nuclear translocation of NF-κB/Rel, AP-1.

Members of the *Mirc11* cistron *miR-23a*, *miR-24-2*, and *miR-27a* have the potentials to silence the translation of hundreds of mRNAs by targeting unique 'seed' sequences present in their 3′ UTR. Using TargetScan 7.1-based *in silico* analyses (http://www.targetscan.org) and by *in silico* predictions, we identified potential target transcripts in the total genome-wide RNA sequencing data from NK cells from listeria-infected WT and *Mirc11*$^{-/-}$ mice based on 'the aggregate probability of conserved targeting' (P_{CT}) (68). Based on the ENCODE Data Coordination Center portal-based whole-genome alignments, we identified transcripts that were differentially expressed in NK cells from *Mirc11*$^{-/-}$ mice compared to WT mice. This genomic data along with additional biochemical analyses indicated that the transcripts encoding A20, Cyld, Cbl-b, and Itch are the direct targets of the *Mirc11* cluster. The 3′ UTR of *Tnfaip3* contained one seed match for *miRNA-23a*-3p between 1664–1671 nts. Incorporation of this sequence into the 3′UTR of luciferase-encoding sequence significantly reduced its translation. 3′ UTR of *Cblb* contained two seed matches between 3216–3236 and 5879–5901 nts targeted by *miR-27a*-3p and *miR-23a*-3p, respectively. Although the proximal seed match sequence for *miR-27a*-3p contained a non-contiguous 13 nucleotides (out of 21) that were complementary, it was unable to block the translation of luciferase. However, the distal sequence that was targeted by *miR-23a*-3p with a 7mer seed match did contribute to translational repression as indicated by the reduction in luciferase activity. The 3′ UTR of *Cyld* contained three sequences between 3842–3864, 4031–4051, and 5979–6000 nts, which were all targeted by *miR-24-2*-3p. Irrespective of the presence of three optimal seed matches, none of these were able to block the translation of luciferase. In this context, it is important to note that *miR-24–1*, the paralog of *miR-24-2*, contains an identical sequence (79). The 3′ UTR of *Itch* contained two seed matches between 2882–2900 and 4649–4669 nts that were targeted by *miR-27a*-3p and *miR-23a*-3p, respectively. While no translational repression was seen from *miR-23a*-3p, incorporation of the target sequences in the 3′UTR of luciferase indicated that the *miR-27a*-3p was able to reduce the translation of luciferase.

Thus, the ability of the *Mirc11* cluster to directly target the transcripts encoding A20, Cyld, Cbl-b, and Itch provides a plausible mechanistic explanation for the reduction in the production of pro-inflammatory factors. Earlier work indicating a high expression level of miRNA-23a in human primary macrophages and its ability to target A20 to repress NF-κB activation and thereby a reduction in IL-6 and TNF-α corroborate our current findings in murine NK cells (112). Deubiquitinating enzymes, such as A20 and Cyld, along with E3 ligases, including Itch and Cbl-b, are the central regulators of TRAF6-NF-kB (80) and TRAF6-AP-1 pathways (113). TRAF6, through its TRAF domain, promotes K63-linked autoubiquitination to function as a scaffold protein to recruit TAB1 and TAB2 (114). TRAF6-mediated K63-polyubiquitination also recruits TAB2 and TAB3 to activate TAK1 (82), which phosphorylates and activates IKKα and IKKβ leading to the nuclear translocation of the NF-κB complex (83). A20 and Cyld are a dual function ubiquitin-editing enzyme that sequentially deubiquitinates the K63- or Met-1 linkages and add K48 linked ubiquitin using their E3 ligase function (84, 115). Both A20 and Cyld can independently associate with Itch and Cyld interacts with Cbl-b to facilitate the removal of

K63 polyubiquitin chains and to add K48 polyubiquitination (36, 85, 116). Although the protein levels of Cyld were augmented in NK cells lacking *Mirc11*, we did not observe a reduction in the activity when its seed-match sequence was placed at the 3′ UTR of luciferase. The post-translational repression of both deubiquitinases and E3 ligases by *Mirc11* is a robust mechanism to dampen the activation of inflammatory responses.

In summary, we have identified a novel post-translational regulatory mechanism of inflammatory responses by microRNAs. The clinical relevance of our findings is highlighted by the evolutionarily conserved expression of the *Mirc11* cistron in human cells including NK cells. Indeed, we have also found that the transduction of pri-miRNAs, an RNA hairpin with mature miRNA, encoding either the individual or all three members of the *Mirc11* cistron was able to increase the production of IFN-γ in purified $CD3\varepsilon^{-}CD56^{+}$ human NK cells. Future work is warranted to define the direct role of the *Mirc11* cluster as underlying genetic susceptibility to inflammatory autoimmune diseases and malignancies.

Contact for Reagents and Resource Sharing

As Lead Contact, Malarkannan is responsible for all reagent and resource requests. Please contact Subramaniam Malarkannan at Subra.Malar@BCW.edu with requests and inquiries.

Experimental Models and Subject Details

Mice and stable cell lines

C57BL/6 mice (WT) were obtained from Jackson Laboratory (Bar Harbor, ME). *Mirc11*$^{-/-}$ mice were generated and backcrossed with C57BL/6 mice for at least ten generations (51). Spleens from *Cyld*$^{-/-}$ *and Itch*$^{-/-}$ mice were a gift from Dr. K Venuprasad Poojary at Baylor Research Institute of Dallas. Spleens from *Tnfaip3*$^{-/-}$ mice were a gift from Dr. Daniel Starczynowski at Cincinnati Children Hospital. All mice were maintained in pathogen-free conditions at the Biological Resource Center (BRC) at the Medical College of Wisconsin (MCW), Milwaukee, WI. Female and male mice between the ages of 6 to 12 weeks were used. All animal protocols and human PBMC usage were approved by the respective institutional IACUC (AUA1512) and IRB committees. EL4, RMA, RMA/S, and YAC-1 cell lines were purchased from ATCC (Rockville, MD) and maintained in RPMI-1640 medium containing 10% heat-inactivated FBS (Life Technologies, Grand Island, NY). Generation of *H60*-expressing EL4 stable cell lines has been described (117). The authenticity of RMA and RMA/S were tested by the levels of MHC-Class I ($H2\text{-}K^{b}$ and $H2\text{-}D^{b}$). $EL4^{H60}$ and EL4 were validated by the presence of cell-surface H60 protein. YAC-1 was tested by the absence of $H\text{-}2^{b}$ and the presence of $H\text{-}2^{a}$ markers. All these cell lines were regularly tested and were negative for mycoplasma.

Antibodies

Antibodies for NK1.1 (PK136), CD3ε (17A2, 145–2C11), NKG2D (A10), CD137 (17b5), CD137L (TKS-1), and anti-human IFN-γ (MG1.2), were obtained from e-Bioscience (San Diego, CA). Anti-Ly49D (4E5) and RIP1 were obtained from BD Pharmingen (San Jose, CA). Antibody for NCR1 (MAB2225) was obtained from R&D Systems (Minneapolis, MN). Antibodies for β-actin (ACTBD11B7), TRAF6 (H-274) and TRAF2 (F-2) were

obtained from Santa Cruz Biotechnology (Dallas, TX). K63-linkage Specific Polyubiquitin (D7A11), K48-linkage Specific Polyubiquitin (D9D5), A20 (#4625), Cbl-b (D3C12), Cyld (#4495) and Itch (D8Q6D) were purchased from Cell Signaling Technologies (Boston, MA). Antibodies for CD45.1 (A20), and CD45.2 (#104) were obtained from BioLegend (San Diego, CA).

Method Details

NK cell preparation

NK cells were purified by single cell suspensions from spleen were passed through nylon wool columns to deplete adherent populations consisting of B cells and macrophages. Nylon wool-non-adherent cells were cultured with 1000 U/ml of IL-2 (NCI-BRB-Preclinical Repository, Maryland, and MD) or 100 ng/ml of IL-15 (Peprotech Inc. Rocky Hill, NJ). The purity of the NK cultures was checked by flow cytometry, and preparations with more than 95 % of $CD3\varepsilon^{-}NK1.1^{+}$ cells were used on day seven of IL-2 or IL-15 cultures.

Cytotoxicity assays

IL-2 or IL-15 cultured NK cells were used as effectors in ^{51}Chromium (Cr)-release assays on day 7. Target cells were labeled with 50 μCi ^{51}Cr (Perkin Elmer, Shelton, CT) in FCS for one hour at 37° C, washed, plated in 96-well U-bottom plates in serial dilutions with effector cells at corresponding ratios, and incubated at 37° C for four hours. Supernatants (100 μl) were then transferred to plastic tubes, and the radioactivity was measured using a 1470 Automatic Gamma Counter (Perkin Elmer Shelton, CT). The amount of specific lysis that occurred in each well was calculated relative to maximum release (MR) by lysing the cells with hydrochloric acid and spontaneous release (SR) of the radioactivity in the media with target cells alone. To calculate percent specific lysis, we used the following formula: 100 × [(experimental counts per minutes (CPM) - SR (average CPM)/(MR (average CPM) - SR (average CPM)] = % specific lysis.

Quantification of cytokines and chemokines

IL-2-cultured NK cells were activated with plate-bound mitogenic antibodies (2.5 μg/ml) against NKG2D (A10), CD137 (17B5), or Ly49D (4E5) for 18 hours. Culture supernatants were collected and analyzed in a Bioplex assay (Bio-Rad, Richmond, CA). As positive controls, IL-2-cultured NK cells were stimulated with one ng/ml of IL-12 (R&D Systems, Minneapolis, MN) and ten ng/ml of IL-18 (MBL, Des Plaines, IL), and the supernatants were analyzed using Bioplex assay. Intracellular IFN-γ was quantified as previously described (118). Briefly, NK cells were activated with plate-bound mAbs in the presence of Brefeldin A. After six h, cells were stained for surface CD3ε and NK1.1, fixed, permeabilized and stained with PE-cy7-conjugated anti-IFN-γ mAb (XMG1.2). For mRNA quantification, NK cells were activated with anti-NKG2D mAb (2.5 μg/ml) for 6 hours, lysed and total RNA was purified using RNeasy Mini Kit (Qiagen, Valencia, CA). Real-time PCR was performed using SYBR green protocol with an ABI7900 HT thermal cycler. Transcript in each sample was assayed in triplicates, and the mean cycle threshold was used to calculate the ***x***-fold change and control changes for each gene. Housekeeping gene ***GAPDH*** was used for global normalization in each experiment.

Immunoblotting

Whole cell lysate (15–20 μg) or nuclear extracts (10 μg) isolated using NE-PER reagent (Pierce Inc., Rockford, IL) were resolved using 10% SDS-PAGE gels, transferred to PVDF membranes, and probed with indicated antibodies. Signals were detected using SuperSignal West Pico Chemiluminescent Substrate (Thermo Scientific, Waltham, MA). The band intensities of phospho-protein were normalized against the respective total protein. The fold changes in phosphorylation following 5 or 20 min of activation was calculated using these normalized values.

Immunoprecipitation

Unstimulated or plate-bound anti-NKG2D mAb mAb (2.5 μg/ml)-activated NK cells were lysed using IP lysis buffer-containing Tris (pH 7.5, 20 mM), NaCl (150 mM), EDTA (1 mM), EGTA (1 mM), Triton X100 (1%), sodium pyrophosphate (2.5 mM), beta-glycerophosphate (1 mM), Sodium orthovanadate (1 mM), leupeptin (1 ug/ml) and PMSF (1 mM). The lysate was centrifuged at 12,000 g for 10 min to remove debris. For immunoprecipitation, 300–500 μg of the lysate was incubated for 1 hour with 2 μg of the indicated antibody at 4° C. 20 μl of Protein G Plus agarose (Santa Cruz Biotechnology, Dallas, TX) was added and incubated overnight at 4° C. Following centrifugation, the supernatant was aspirated, and the beads were washed with the IP lysis buffer. SDS-sample buffer (6X, reducing, BP-111R, Boston BioProducts, Boston, MA) diluted to 1X concentration with the IP lysis buffer was added to the bead pellet and denatured at 95° C for 10 min. The samples were electrophoresed using 10% SDS-PAGE gel.

Electrophoretic mobility shift assay for NF-κB and AP-1

IL-2-cultured NK cells (3×10^6) from WT and *Mirc11*-deficient mice were stimulated with anti- NKG2D mAb (2.5 μg/ml) for 40 min and then prepared for nuclear extracts. Nuclear extracts were incubated with ^{32}P-labeled NF-κB or AP-1 probe (NF-κB probe: 5′-AGTTGAGGGGACTTTCCCAGGC-3′; AP-1 probe: 5′-CGCTTGATGACTCAGCCGGAA-3; Santa Cruz Biotechnology, Dallas, TX) for 15 min at room temperature, resolved on a 4 % polyacrylamide gel at 4° C, and exposed to X-ray film.

Preparation of cytoplasmic and nuclear extracts

IL-2-cultured NK cells (3×10^6) from WT and *Mirc11*$^{-/-}$ mice were stimulated with anti-NKG2D mAb (2.5 μg/ml) for 40 min. The cells were collected and suspended in 100 ml cold buffer A (10 mM HEPES pH 7.9, 10 mM KCl, 0.2 mM EDTA, 1 mM DTT, 3 mg/ml aprotinin, 2 mg/ml Pepstatin, and 1 mg/ml leupeptin). After incubation on ice for 15 min, Nonidet P-40 was added to a final concentration of 0.5 %. The mixtures were vortexed for 10 sec and spun at 16,000 g for 30 sec. The supernatants were collected as the cytoplasmic extracts. The pellets were washed with Buffer A once and resuspended in 50 ml Buffer B (20 mM HEPES pH 7.9, 400 mM NaCl, 2 mM EDTA, 1 mM DTT, 3 mg/ml aprotinin, 2 mg/ml Pepstatin, and 1 mg/ml leupeptin), followed by incubation on ice for 15 min. The mixtures were spun at 16,000 g for 5 min, and the supernatants were collected as the nuclear extracts.

Flow cytometry

NK cells, stable cell lines or single cell preparations from spleen, lung, liver or BM were stained with fluorescent-labeled monoclonal antibodies (mAbs) in 1 % FCS-PBS as described. One million events were analyzed for each sample. Standard flow cytometry analyses were performed in LSR-II or MACSQuant instruments at the Blood Center of Wisconsin-Flow Cytometry Core Facility and analyzed with FACS Diva software (BD, Franklin Lakes, NJ) or FlowJo (Ashland, OR).

RNA isolation and quantitative analyses for the members of the *Mirc11* cluster

For extraction of miRNAs, TRIzol (Invitrogen, San Diego CA) was used. DNase I-treated total RNA (8 ng) was subjected to qRT-PCR analysis using TaqMan miR Reverse Transcription Kit (Applied Biosystems, Foster City CA). The *miR-23a*, *miR-24-2*, and *miR-27a* were detected and quantified by using specific miRNA primers from Ambion. Expression levels of mature miRNAs were evaluated using comparative Ct method (2- ΔCt). Transcript levels normalized with small nucleolar RNA 202.

microRNA target prediction and luciferase reporter assay

Miranda (www.microrna.org/microrna/home.do) and TargetScan (www.targetscan.org) were used as a first and second source to identify potential targets for *miR-23a*, *miR-24-2*, and *miR-27a*. To validate that *A20, Cblb, Itch, and Cyld* are the targets of the *Mirc11* cluster, binding site sequences of these target genes were cloned into the psiCHECK vector in HEK293T cells. HEK293T cells were then co-transfected with the luciferase reporter constructs with ten nmol/L of *pre-miR-23a*, *pre-miR-24-2*, *pre-miR-27a*, or control microRNA. Transfection was done using Lipofectamine 2000 (Invitrogen) in OPTIMEM (Invitrogen) medium. After 48 h, the cells were harvested, and the luciferase signals were measured with the Luciferase Reporter Assay System (Promega, Madison WI).

Lentiviral vectors and constructs

Lenti-miR vectors (System Biosciences, Palo Alto CA) were purchased and used to produce mature *miRNA-23a*, *miRNA-24-2*, and *miRNA −27a* individually or together from CMV promoter with GFP reporter to monitor miRNA-expressing cells. Transduced NK cells (10^5) were co-cultured with K562 (10^5) for four hours and intracellular IFN-γ expression has been quantified by flow cytometry.

Listeria monocytogenes infection

For infection of mice, *Listeria monocytogenes* was grown to stationary phase, aliquoted, tittered, and stored at 80° C. Before injection, bacteria were thawed on ice, grown to early exponential phase in brain-heart infusion broth, and diluted in PBS. The LD_{50} of *L. monocytogenes* strain 10403S is 2×10^5 CFU in C57BL/6 mice. For infections, a dose of 10^4 or 2×10^4 was suspended in 200 μl of PBS and injected through retro-orbital of 8–12 weeks old mice. Mice were monitored daily, and 48 or 72 h later were sacrificed for further experiments. Spleens were processed into single-cell suspensions for staining and flow cytometry as well as RNA extraction for RNA-seq experiment. Livers were processed with a tissue homogenizer, and tissue extracts were plated for CFU calculation.

RNA sequencing

Total RNA was extracted from splenic CD3ε^{-}NK1.1^{+} NK cells from WT and *Mirc11*$^{-/-}$ mice using Trizol before and after challenging them with 2 × 10^4 CFU of *L. monocytogenes* (n = 3/group), followed by poly-A-purification, transcription, and chemical fragmentation using Illumina's TruSeq RNA library kit using the manufacturer's protocol (Illumina Inc., San Diego, CA). Individual libraries were prepared for each NK cell preparation, indexed for multiplexing, and then sequenced either on NextSeq500 (Anti-NKG2D mAb activation) or an Illumina HiSeq2500 (NK cells derived following *L. monocytogenes* infections. The Trim Galore program (v0.4.1) was used to trim bases with a Phred quality score <20 [https://www.bioinformatics.babraham.ac.uk/projects/trim_galore/<https://urldefense.proofpoint.com/v2/url?u=https3A__www.bioinformatics.babraham.ac.uk_projects_trim5Fgalore_&d=DwQFAw&c=aFamLAsxMIDYjNglYHTMV0iqFn3z4pVFYPQkjgspw4Y&r=S5gLYQA2eD6OkaEXHZBgag&m=SrvltlssjduHvUOw7wzDOJA5YPyFgFxSh5PXKzAWTLQ&s=A49CtYVs5efaJJuFDrNg3dKMJgiCPn-xEgLbqk_ZYiE&e=>] and only reads with a Phred quality score equal or higher than 20 were taken for analyses. The RSEM program function "rsem-prepare-reference" (v1.3.0) was used to extract the transcript sequences from the mouse genome (Build GRCm38) (119) and to generate Bowtie2 indices (Bowtie2 v2.2.8) (120), followed by reading alignment using the "RSEM-calculate-expression" function. Differential expression analysis was performed using the Bioconductor package DESeq2 version 1.12.4 (121) to compute Log_2 fold changes and false discovery rate-adjusted p-values. Statistical significance was determined at a false discovery rate threshold of 0.05. Data were analyzed for molecular and functional pathway enrichment using Ingenuity Pathway Analysis (IPA; Qiagen, Redwood City, CA, USA). IPA Informatics software tool was used by classifying the data set into gene ontology (GO) categories with a false discovery rate (FDR) of 0.01% based on biological process (BP) and molecular function (MF) categories with a minimum of two-fold change restriction. We interrogated a B-cell regulatory networks (http://califano.c2b2.columbia.edu/networks/) with the gene expression profiles among stimulated WT and *Mirc11*$^{-/-}$ NK cells samples, to identify the regulon of each gene-of-interest. This network analysis was carried out using the R Bioconductor package DeMAND (https://bioconductor.org/packages/release/bioc/html/DeMAND.html). The network analysis was carried out as the following: (1) estimation of the dysregulation of an edge in the human B-cell regulatory network and (2) the estimation of the dysregulation of a gene.

B16F10 lung metastasis

B16F10 melanoma cells growing in log phase were harvested and suspended in PBS. 2 × 10^5, or 10^6 cells were injected into mice through the retro-orbital or tail vein. Fourteen days later post-injection, the recipient mice were euthanized, 10 ml PBS was used for a right ventricular flush, and the lungs were excised. Each set of lungs were photographed, and the lung nodules were counted. For early B16F10 metastasis formation, 10^6 cells were injected, and the lungs were analyzed on day 7 of post-injection. For optimal metastasis, 2 × 10^5 B16F10 cells were injected, and the lungs were analyzed on day 14 of post-injection. Tumor nodules in the lung were counted in a blinded manner. Lungs were fixed in 10% (*v/v*) neutral buffered formalin for 24–72 h. After fixing, tissues were dehydrated through graded ethanol, cleared with xylene, paraffin infiltrated (Sakura VIP5 automated tissue processor)

and embedded into tissue blocks. Tissue blocks were cut at 4 μm and mounted on poly-L-lysine coated slides. Sections were deparaffinized with xylene, rehydrated, and stained with Hematoxylin and Eosin on an automated staining platform (Sakura Prisma). Stained slides were scanned using a Hamamatsu Slide scanner and viewed using NDPiView software.

Experimental data and statistical analysis

Total sample numbers were determined based on previous studies that used similar transgenic mouse models with comparable functional defects. Statistical analyses were performed using paired, two sample equal or unequal variance. Student's t-test depending on the type of data. P values of ≤ 0.05 were considered significant. Normal distribution of sample variance was assumed on the basis of earlier studies with data sets similar to the current study.

Supplementary Material

Refer to Web version on PubMed Central for supplementary material.

Acknowledgments.

We thank Lucia Sammarco and her Lulu's Lemonade Stand for inspiration, motivation, and support. This work was supported in part by NIH R01 AI102893 (S.M.) and NCI R01 CA179363 (S.M. and M.S.T.); Alex Lemonade Stand Foundation (S.M.); HRHM Program of MACC Fund/Children's Hospital of Wisconsin (S.M.), Nicholas Family Foundation (S.M.); Gardetto Family (S.M.); MCW-Cancer Center-Large Seed Grant (S.M. & M.S.T.); MACC Fund/Children's Hospital of Wisconsin (M.S.T. and S.M.); Ann's Hope Melanoma Foundation (S.M. and M.S.T.); and Advancing Healthier Wisconsin (S.M. & M.R.).

References

1. Yokoyama WM & Plougastel BF (2003) Immune functions encoded by the natural killer gene complex. Nat. Rev. Immunol 3(4):304–316. [PubMed: 12669021]
2. Eberl G, Di Santo JP, & Vivier E (2015) The brave new world of innate lymphoid cells. Nat. Immunol 16(1):1–5. [PubMed: 25521670]
3. Bryceson YT & Long EO (2008) Line of attack: NK cell specificity and integration of signals. Curr. Opin. Immunol 20(3):344–352. [PubMed: 18439809]
4. Bauer S, et al. (1999) Activation of NK cells and T cells by NKG2D, a receptor for stress-inducible MICA. Science 285(5428):727–729. [PubMed: 10426993]
5. Lanier LL, Corliss B, Wu J, & Phillips JH (1998) Association of DAP12 with activating CD94/NKG2C NK cell receptors. Immunity 8(6):693–701. [PubMed: 9655483]
6. Wu J, Cherwinski H, Spies T, Phillips JH, & Lanier LL (2000) DAP10 and DAP12 form distinct, but functionally cooperative, receptor complexes in natural killer cells. J. Exp. Med 192(7):1059–1068. [PubMed: 11015446]
7. Diefenbach A, et al. (2002) Selective associations with signaling proteins determine stimulatory versus costimulatory activity of NKG2D. Nat. Immunol 3(12):1142–1149. [PubMed: 12426565]
8. Westgaard IH, et al. (2004) Rat NKp46 activates natural killer cell cytotoxicity and is associated with FcepsilonRIgamma and CD3zeta. J. Leukoc. Biol 76(6):1200–1206. [PubMed: 15356098]
9. Billadeau DD, Upshaw JL, Schoon RA, Dick CJ, & Leibson PJ (2003) NKG2D-DAP10 triggers human NK cell-mediated killing via a Syk-independent regulatory pathway. Nat. Immunol 4(6):557–564. [PubMed: 12740575]
10. Dong Z, et al. (2012) The adaptor SAP controls NK cell activation by regulating the enzymes Vav-1 and SHIP-1 and by enhancing conjugates with target cells. Immunity 36(6):974–985. [PubMed: 22683124]

11. Binstadt BA, et al. (1996) Sequential involvement of Lck and SHP-1 with MHC-recognizing receptors on NK cells inhibits FcR-initiated tyrosine kinase activation. Immunity 5(6):629–638. [PubMed: 8986721]
12. Guo H, Samarakoon A, Vanhaesebroeck B, & Malarkannan S (2008) The p110 delta of PI3K plays a critical role in NK cell terminal maturation and cytokine/chemokine generation. J Exp. Med 205(10):2419–2435. [PubMed: 18809712]
13. Tassi I, et al. (2007) p110gamma and p110delta Phosphoinositide 3-Kinase Signaling Pathways Synergize to Control Development and Functions of Murine NK Cells. Immunity 27(2):214–227. [PubMed: 17723215]
14. Awasthi A, et al. (2008) Deletion of PI3K-p85alpha gene impairs lineage commitment, terminal maturation, cytokine generation and cytotoxicity of NK cells. Genes Immun 9(6):522–535. [PubMed: 18548087]
15. Giurisato E, et al. (2007) Phosphatidylinositol 3-kinase activation is required to form the NKG2D immunological synapse. Mol. Cell Biol 27(24):8583–8599. [PubMed: 17923698]
16. Tassi I, et al. (2005) Phospholipase C-gamma 2 is a critical signaling mediator for murine NK cell activating receptors. J. Immunol 175(2):749–754. [PubMed: 16002670]
17. Regunathan J, et al. (2006) Differential and nonredundant roles of phospholipase Cgamma2 and phospholipase Cgamma1 in the terminal maturation of NK cells. J. Immunol 177(8):5365–5376. [PubMed: 17015722]
18. Rajasekaran K, et al. (2013) Signaling by Fyn-ADAP via the Carma1-Bcl-10-MAP3K7 signalosome exclusively regulates inflammatory cytokine production in NK cells. Nat. Immunol 14(11):1127–1136. [PubMed: 24036998]
19. Gerbec ZJ, Thakar MS, & Malarkannan S (2015) The Fyn-ADAP Axis: Cytotoxicity Versus Cytokine Production in Killer Cells. Front Immunol 6:472. [PubMed: 26441977]
20. Tassi I, et al. (2008) NK cell-activating receptors require PKC-theta for sustained signaling, transcriptional activation, and IFN-gamma secretion. Blood 112(10):4109–4116. [PubMed: 18784374]
21. Gross O, et al. (2008) Multiple ITAM-coupled NK-cell receptors engage the Bcl10/Malt1 complex via Carma1 for NF-kappaB and MAPK activation to selectively control cytokine production. Blood 112(6):2421–2428. [PubMed: 18192506]
22. Malarkannan S, et al. (2007) Bcl10 plays a divergent role in NK cell-mediated cytotoxicity and cytokine generation. J. Immunol 179(6):3752–3762. [PubMed: 17785812]
23. Rajasekaran K, et al. (2011) Transforming Growth Factor-{beta}-activated Kinase 1 Regulates Natural Killer Cell-mediated Cytotoxicity and Cytokine Production. J Biol. Chem 286(36):31213–31224. [PubMed: 21771792]
24. Malynn BA & Ma A (2010) Ubiquitin makes its mark on immune regulation. Immunity 33(6):843–852. [PubMed: 21168777]
25. Kwon HJ, et al. (2016) Stepwise phosphorylation of p65 promotes NF-kappaB activation and NK cell responses during target cell recognition. Nat Commun 7:11686. [PubMed: 27221592]
26. Nausch N, et al. (2006) Cutting edge: the AP-1 subunit JunB determines NK cell-mediated target cell killing by regulation of the NKG2D-ligand RAE-1epsilon. J Immunol 176(1):7–11. [PubMed: 16365389]
27. Rajasekaran K, et al. (2016) Signaling in Effector Lymphocytes: Insights toward Safer Immunotherapy. Front Immunol 7:176. [PubMed: 27242783]
28. Huntington ND, Xu Y, Nutt SL, & Tarlinton DM (2005) A requirement for CD45 distinguishes Ly49D-mediated cytokine and chemokine production from killing in primary natural killer cells. J. Exp. Med 201(9):1421–1433. [PubMed: 15867094]
29. Hesslein DG, et al. (2011) Differential requirements for CD45 in NK-cell function reveal distinct roles for Syk-family kinases. Blood 117(11):3087–3095. [PubMed: 21245479]
30. Vely F, et al. (1997) Differential association of phosphatases with hematopoietic co-receptors bearing immunoreceptor tyrosine-based inhibition motifs. Eur. J. Immunol 27(8):1994–2000. [PubMed: 9295037]

31. Wang LL, Blasioli J, Plas DR, Thomas ML, & Yokoyama WM (1999) Specificity of the SH2 domains of SHP-1 in the interaction with the immunoreceptor tyrosine-based inhibitory motif-bearing receptor gp49B. J. Immunol 162(3):1318–1323. [PubMed: 9973385]
32. Kim S, et al. (2005) Licensing of natural killer cells by host major histocompatibility complex class I molecules. Nature 436(7051):709–713. [PubMed: 16079848]
33. Eissmann P, et al. (2005) Molecular basis for positive and negative signaling by the natural killer cell receptor 2B4 (CD244). Blood 105(12):4722–4729. [PubMed: 15713798]
34. Long EO, Kim HS, Liu D, Peterson ME, & Rajagopalan S (2013) Controlling natural killer cell responses: integration of signals for activation and inhibition. Annu Rev Immunol 31:227–258. [PubMed: 23516982]
35. Duwel M, et al. (2009) A20 negatively regulates T cell receptor signaling to NF-kappaB by cleaving Malt1 ubiquitin chains. J. Immunol 182(12):7718–7728. [PubMed: 19494296]
36. Shembade N, et al. (2008) The E3 ligase Itch negatively regulates inflammatory signaling pathways by controlling the function of the ubiquitin-editing enzyme A20. Nat Immunol 9(3):254–262. [PubMed: 18246070]
37. Fang D & Liu YC (2001) Proteolysis-independent regulation of PI3K by Cbl-b-mediated ubiquitination in T cells. Nat. Immunol 2(9):870–875. [PubMed: 11526404]
38. Reiley WW, et al. (2007) Deubiquitinating enzyme CYLD negatively regulates the ubiquitin-dependent kinase Tak1 and prevents abnormal T cell responses. J. Exp. Med 204(6):1475–1485. [PubMed: 17548520]
39. Guven-Maiorov E, Keskin O, Gursoy A, & Nussinov R (2015) A Structural View of Negative Regulation of the Toll-like Receptor-Mediated Inflammatory Pathway. Biophys J 109(6):1214–1226. [PubMed: 26276688]
40. Bartel DP (2004) MicroRNAs: genomics, biogenesis, mechanism, and function. Cell 116(2):281–297. [PubMed: 14744438]
41. Lewis BP, Burge CB, & Bartel DP (2005) Conserved seed pairing, often flanked by adenosines, indicates that thousands of human genes are microRNA targets. Cell 120(1):15–20. [PubMed: 15652477]
42. Vaucheret H, Vazquez F, Crete P, & Bartel DP (2004) The action of ARGONAUTE1 in the miRNA pathway and its regulation by the miRNA pathway are crucial for plant development. Genes Dev 18(10):1187–1197. [PubMed: 15131082]
43. Bartel DP (2018) Metazoan MicroRNAs. Cell 173(1):20–51. [PubMed: 29570994]
44. Kuchen S, et al. (2010) Regulation of microRNA expression and abundance during lymphopoiesis. Immunity 32(6):828–839. [PubMed: 20605486]
45. Naveed A, Ur-Rahman S, Abdullah S, & Naveed MA (2017) A Concise Review of MicroRNA Exploring the Insights of MicroRNA Regulations in Bacterial, Viral and Metabolic Diseases. Mol Biotechnol 59(11–12):518–529. [PubMed: 28884294]
46. Chhabra R, Dubey R, & Saini N (2010) Cooperative and individualistic functions of the microRNAs in the miR-23a~27a~24-2 cluster and its implication in human diseases. Mol Cancer 9:232. [PubMed: 20815877]
47. Cho S, et al. (2016) miR-23 approximately 27 approximately 24 clusters control effector T cell differentiation and function. J Exp Med 213(2):235–249. [PubMed: 26834155]
48. Pua HH, et al. (2016) MicroRNAs 24 and 27 Suppress Allergic Inflammation and Target a Network of Regulators of T Helper 2 Cell-Associated Cytokine Production. Immunity 44(4):821–832. [PubMed: 26850657]
49. Kondo M (2010) Lymphoid and myeloid lineage commitment in multipotent hematopoietic progenitors. Immunol Rev 238(1):37–46. [PubMed: 20969583]
50. Kurkewich JL, et al. (2017) The miR-23a~27a~24-2 microRNA cluster buffers transcription and signaling pathways during hematopoiesis. PLoS Genet 13(7):e1006887. [PubMed: 28704388]
51. Kurkewich JL, et al. (2016) The mirn23a microRNA cluster antagonizes B cell development. J Leukoc Biol 100(4):665–677. [PubMed: 27084569]
52. Kim S, et al. (2002) In vivo developmental stages in murine natural killer cell maturation. Nat. Immunol 3(6):523–528. [PubMed: 12006976]

53. Rosmaraki EE, et al. (2001) Identification of committed NK cell progenitors in adult murine bone marrow. Eur. J. Immunol 31(6):1900–1909. [PubMed: 11433387]
54. Vosshenrich CA, et al. (2005) Roles for common cytokine receptor gamma-chain-dependent cytokines in the generation, differentiation, and maturation of NK cell precursors and peripheral NK cells in vivo. J. Immunol 174(3):1213–1221. [PubMed: 15661875]
55. Robbins SH, et al. (2002) Cutting edge: inhibitory functions of the killer cell lectin-like receptor G1 molecule during the activation of mouse NK cells. J. Immunol 168(6):2585–2589. [PubMed: 11884419]
56. Guan H, Nagarkatti PS, & Nagarkatti M (2007) Blockade of hyaluronan inhibits IL-2-induced vascular leak syndrome and maintains effectiveness of IL-2 treatment for metastatic melanoma. J Immunol 179(6):3715–3723. [PubMed: 17785808]
57. Orange JS, et al. (2011) IL-2 induces a WAVE2-dependent pathway for actin reorganization that enables WASp-independent human NK cell function. J Clin Invest 121(4):1535–1548. [PubMed: 21383498]
58. Vivier E, Ugolini S, & Nunes JA (2013) ADAPted secretion of cytokines in NK cells. Nat. Immunol 14(11):1108–1110. [PubMed: 24145781]
59. Takeda K, et al. (1998) Defective NK cell activity and Th1 response in IL-18-deficient mice. Immunity 8(3):383–390. [PubMed: 9529155]
60. Nakahira M, et al. (2001) An absolute requirement for STAT4 and a role for IFN-gamma as an amplifying factor in IL-12 induction of the functional IL-18 receptor complex. J Immunol 167(3):1306–1312. [PubMed: 11466347]
61. Nakahira M, et al. (2002) Synergy of IL-12 and IL-18 for IFN-gamma gene expression: IL-12-induced STAT4 contributes to IFN-gamma promoter activation by up-regulating the binding activity of IL-18-induced activator protein 1. J Immunol 168(3):1146–1153. [PubMed: 11801649]
62. Thale C & Kiderlen AF (2005) Sources of interferon-gamma (IFN-gamma) in early immune response to Listeria monocytogenes. Immunobiology 210(9):673–683. [PubMed: 16323704]
63. Teixeira HC & Kaufmann SH (1994) Role of NK1.1+ cells in experimental listeriosis. NK1+ cells are early IFN-gamma producers but impair resistance to Listeria monocytogenes infection. J. Immunol 152(4):1873–1882. [PubMed: 8120395]
64. Teixeira HC & Kaufmann SH (1994) Role of NK1.1+ cells in experimental listeriosis. NK1+ cells are early IFN-gamma producers but impair resistance to Listeria monocytogenes infection. J Immunol 152(4):1873–1882. [PubMed: 8120395]
65. Shegarfi H, Rolstad B, Kane KP, & Nestvold J (2018) Listeria monocytogenes infection differentially affects expression of ligands for NK cells and NK cell responses, depending on the cell type infected. J Leukoc Biol 103(3):591–599. [PubMed: 27106671]
66. Fidler IJ, Gersten DM, & Budmen MB (1976) Characterization in vivo and in vitro of tumor cells selected for resistance to syngeneic lymphocyte-mediated cytotoxicity. Cancer Res 36(9 pt.1):3160–3165. [PubMed: 975082]
67. Takeda K, et al. (2011) IFN-gamma production by lung NK cells is critical for the natural resistance to pulmonary metastasis of B16 melanoma in mice. J. Leukoc. Biol 90(4):777–785. [PubMed: 21712396]
68. Friedman RC, Farh KK, Burge CB, & Bartel DP (2009) Most mammalian mRNAs are conserved targets of microRNAs. Genome Res 19(1):92–105. [PubMed: 18955434]
69. Rosenberger CM, Clark AE, Treuting PM, Johnson CD, & Aderem A (2008) ATF3 regulates MCMV infection in mice by modulating IFN-gamma expression in natural killer cells. Proc Natl Acad Sci U S A 105(7):2544–2549. [PubMed: 18268321]
70. Li P, et al. (2012) BATF-JUN is critical for IRF4-mediated transcription in T cells. Nature 490(7421):543–546. [PubMed: 22992523]
71. Glasmacher E, et al. (2012) A genomic regulatory element that directs assembly and function of immune-specific AP-1-IRF complexes. Science 338(6109):975–980. [PubMed: 22983707]
72. Schroeder TM, Jensen ED, & Westendorf JJ (2005) Runx2: a master organizer of gene transcription in developing and maturing osteoblasts. Birth Defects Res C Embryo Today 75(3):213–225. [PubMed: 16187316]

73. Chopin M, et al. (2016) RUNX2 Mediates Plasmacytoid Dendritic Cell Egress from the Bone Marrow and Controls Viral Immunity. Cell Rep 15(4):866–878. [PubMed: 27149837]
74. Sun L, Deng L, Ea CK, Xia ZP, & Chen ZJ (2004) The TRAF6 ubiquitin ligase and TAK1 kinase mediate IKK activation by BCL10 and MALT1 in T lymphocytes. Mol. Cell 14(3):289–301. [PubMed: 15125833]
75. Newton K & Dixit VM (2003) Mice lacking the CARD of CARMA1 exhibit defective B lymphocyte development and impaired proliferation of their B and T lymphocytes. Curr. Biol 13(14):1247–1251. [PubMed: 12867037]
76. Hayden MS & Ghosh S (2012) NF-kappaB, the first quarter-century: remarkable progress and outstanding questions. Genes Dev 26(3):203–234. [PubMed: 22302935]
77. Woo JH, et al. (2015) Elucidating Compound Mechanism of Action by Network Perturbation Analysis. Cell 162(2):441–451. [PubMed: 26186195]
78. Chen ZJ (2012) Ubiquitination in signaling to and activation of IKK. Immunol Rev 246(1):95–106. [PubMed: 22435549]
79. Bang C, Fiedler J, & Thum T (2012) Cardiovascular importance of the microRNA-23/27/24 family. Microcirculation 19(3):208–214. [PubMed: 22136461]
80. Baud V, et al. (1999) Signaling by proinflammatory cytokines: oligomerization of TRAF2 and TRAF6 is sufficient for JNK and IKK activation and target gene induction via an amino-terminal effector domain. Genes Dev 13(10):1297–1308. [PubMed: 10346818]
81. Venuprasad K, Zeng M, Baughan SL, & Massoumi R (2015) Multifaceted role of the ubiquitin ligase Itch in immune regulation. Immunol Cell Biol 93(5):452–460. [PubMed: 25582340]
82. Ohtake F, Saeki Y, Ishido S, Kanno J, & Tanaka K (2016) The K48-K63 Branched Ubiquitin Chain Regulates NF-kappaB Signaling. Mol Cell 64(2):251–266. [PubMed: 27746020]
83. Wang C, et al. (2001) TAK1 is a ubiquitin-dependent kinase of MKK and IKK. Nature 412(6844):346–351. [PubMed: 11460167]
84. Hitotsumatsu O, et al. (2008) The ubiquitin-editing enzyme A20 restricts nucleotide-binding oligomerization domain containing 2-triggered signals. Immunity 28(3):381–390. [PubMed: 18342009]
85. Ahmed N, et al. (2011) The E3 ligase Itch and deubiquitinase Cyld act together to regulate Tak1 and inflammation. Nat Immunol 12(12):1176–1183. [PubMed: 22057290]
86. Xu M, Skaug B, Zeng W, & Chen ZJ (2009) A ubiquitin replacement strategy in human cells reveals distinct mechanisms of IKK activation by TNFalpha and IL-1beta. Mol. Cell 36(2):302–314. [PubMed: 19854138]
87. Liu X, et al. (2012) Identification of microRNA transcriptome involved in human natural killer cell activation. Immunol Lett 143(2):208–217. [PubMed: 22701882]
88. Fehniger TA, et al. (2010) Next-generation sequencing identifies the natural killer cell microRNA transcriptome. Genome Res 20(11):1590–1604. [PubMed: 20935160]
89. Liang T, Yu J, Liu C, & Guo L (2014) An exploration of evolution, maturation, expression and function relationships in mir-23 approximately 27 approximately 24 cluster. PLoS One 9(8):e106223. [PubMed: 25157521]
90. Bezman NA, et al. (2010) Distinct requirements of microRNAs in NK cell activation, survival, and function. J Immunol 185(7):3835–3846. [PubMed: 20805417]
91. Sullivan RP, et al. (2012) MicroRNA-deficient NK cells exhibit decreased survival but enhanced function. J Immunol 188(7):3019–3030. [PubMed: 22379033]
92. Cichocki F, et al. (2011) Cutting edge: microRNA-181 promotes human NK cell development by regulating Notch signaling. J Immunol 187(12):6171–6175. [PubMed: 22084432]
93. Bezman NA, Chakraborty T, Bender T, & Lanier LL (2011) miR-150 regulates the development of NK and iNKT cells. J Exp Med 208(13):2717–2731. [PubMed: 22124110]
94. Kim N, et al. (2014) MicroRNA-150 regulates the cytotoxicity of natural killers by targeting perforin-1. J. Allergy Clin. Immunol 134(1):195–203. [PubMed: 24698324]
95. Sullivan RP, et al. (2015) MicroRNA-15/16 Antagonizes Myb To Control NK Cell Maturation. J Immunol 195(6):2806–2817. [PubMed: 26268657]

96. Presnell SR, Al-Attar A, Cichocki F, Miller JS, & Lutz CT (2015) Human natural killer cell microRNA: differential expression of MIR181A1B1 and MIR181A2B2 genes encoding identical mature microRNAs. Genes Immun 16(1):89–98. [PubMed: 25410655]

97. Kim TD, et al. (2011) Human microRNA-27a* targets Prf1 and GzmB expression to regulate NK-cell cytotoxicity. Blood 118(20):5476–5486. [PubMed: 21960590]

98. Aquino-Lopez A, Senyukov VV, Vlasic Z, Kleinerman ES, & Lee DA (2017) Interferon Gamma Induces Changes in Natural Killer (NK) Cell Ligand Expression and Alters NK Cell-Mediated Lysis of Pediatric Cancer Cell Lines. Front Immunol 8:391. [PubMed: 28428785]

99. Barber DF, Faure M, & Long EO (2004) LFA-1 contributes an early signal for NK cell cytotoxicity. J. Immunol 173(6):3653–3659. [PubMed: 15356110]

100. Malarkannan S, et al. (1998) The molecular and functional characterization of a dominant minor H antigen, H60. J. Immunol 161(7):3501–3509. [PubMed: 9759870]

101. Malarkannan S, et al. (2000) Differences that matter: major cytotoxic T cell-stimulating minor histocompatibility antigens. Immunity 13(3):333–344. [PubMed: 11021531]

102. Samarakoon A, Chu H, & Malarkannan S (2009) Murine NKG2D ligands: “double, double toil and trouble”. Mol Immunol 46(6):1011–1019. [PubMed: 19081632]

103. Lin R, et al. (2014) Targeting miR-23a in CD8+ cytotoxic T lymphocytes prevents tumor-dependent immunosuppression. J Clin Invest 124(12):5352–5367. [PubMed: 25347474]

104. Dunn PL & North RJ (1991) Early gamma interferon production by natural killer cells is important in defense against murine listeriosis. Infect Immun 59(9):2892–2900. [PubMed: 1679040]

105. Zhang B, et al. (2016) MicroRNA-23a Curbs Necrosis during Early T Cell Activation by Enforcing Intracellular Reactive Oxygen Species Equilibrium. Immunity 44(3):568–581. [PubMed: 26921109]

106. Long EO (2007) Ready for prime time: NK cell priming by dendritic cells. Immunity 26(4):385–387. [PubMed: 17459805]

107. Lucas M, Schachterle W, Oberle K, Aichele P, & Diefenbach A (2007) Dendritic cells prime natural killer cells by trans-presenting interleukin 15. Immunity 26(4):503–517. [PubMed: 17398124]

108. Koka R, et al. (2003) Interleukin (IL)-15R[alpha]-deficient natural killer cells survive in normal but not IL-15R[alpha]-deficient mice. J. Exp. Med 197(8):977–984. [PubMed: 12695489]

109. Koka R, et al. (2004) Cutting edge: murine dendritic cells require IL-15R alpha to prime NK cells. J. Immunol 173(6):3594–3598. [PubMed: 15356102]

110. Netea MG, et al. (2017) A guiding map for inflammation. Nat Immunol 18(8):826–831. [PubMed: 28722720]

111. Rothschild DE, McDaniel DK, Ringel-Scaia VM, & Allen IC (2018) Modulating inflammation through the negative regulation of NF-kappaB signaling. J Leukoc Biol.

112. Peng P, Li Z, & Liu X (2015) Reduced Expression of miR-23a Suppresses A20 in TLR-stimulated Macrophages. Inflammation 38(5):1787–1793. [PubMed: 25832477]

113. Shim JH, et al. (2005) TAK1, but not TAB1 or TAB2, plays an essential role in multiple signaling pathways in vivo. Genes Dev 19(22):2668–2681. [PubMed: 16260493]

114. Ye H, et al. (2002) Distinct molecular mechanism for initiating TRAF6 signalling. Nature 418(6896):443–447. [PubMed: 12140561]

115. Hrdinka M, et al. (2016) CYLD Limits Lys63- and Met1-Linked Ubiquitin at Receptor Complexes to Regulate Innate Immune Signaling. Cell Rep 14(12):2846–2858. [PubMed: 26997266]

116. Sanchez-Quiles V, et al. (2017) Cylindromatosis Tumor Suppressor Protein (CYLD) Deubiquitinase is Necessary for Proper Ubiquitination and Degradation of the Epidermal Growth Factor Receptor. Mol Cell Proteomics 16(8):1433–1446. [PubMed: 28572092]

117. Regunathan J, Chen Y, Wang D, & Malarkannan S (2005) NKG2D receptor-mediated NK cell function is regulated by inhibitory Ly49 receptors. Blood 105(1):233–240. [PubMed: 15328154]

118. Abel AM, et al. (2018) IQ Domain-Containing GTPase-Activating Protein 1 Regulates Cytoskeletal Reorganization and Facilitates NKG2D-Mediated Mechanistic Target of Rapamycin

Complex 1 Activation and Cytokine Gene Translation in Natural Killer Cells. Front Immunol 9:1168. [PubMed: 29892299]

119. Li B & Dewey CN (2011) RSEM: accurate transcript quantification from RNA-Seq data with or without a reference genome. BMC Bioinformatics 12:323. [PubMed: 21816040]
120. Langmead B & Salzberg SL (2012) Fast gapped-read alignment with Bowtie 2. Nat Methods 9(4):357–359. [PubMed: 22388286]
121. Love MI, Huber W, & Anders S (2014) Moderated estimation of fold change and dispersion for RNA-seq data with DESeq2. Genome Biol 15(12):550. [PubMed: 25516281]

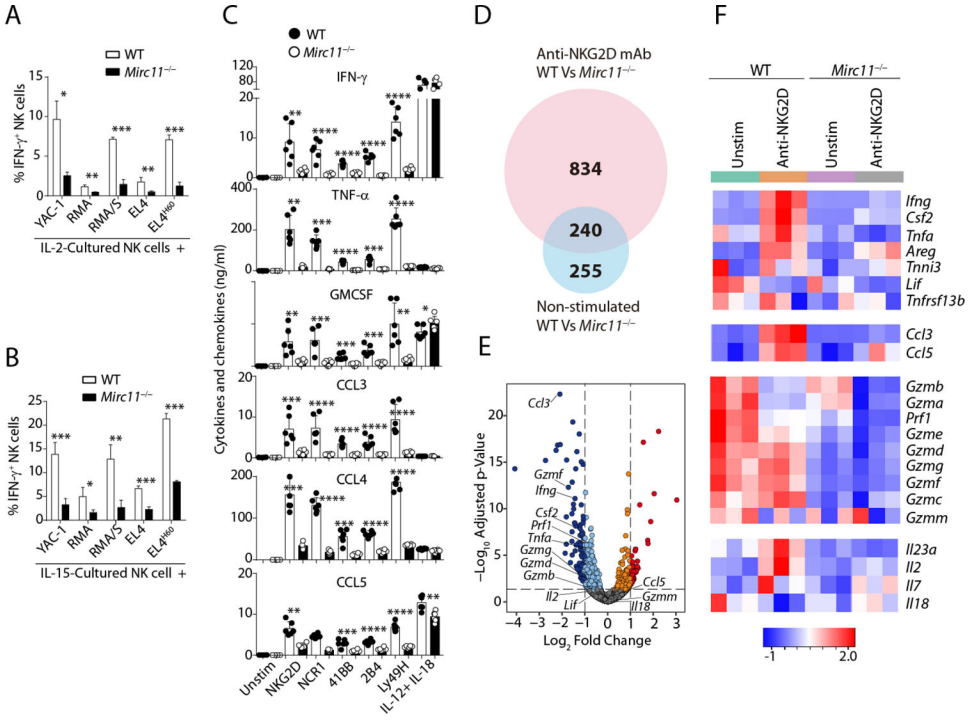

Figure 1. Lack of *Mirc11* significantly reduces NK cell-mediated cytokine production *in vitro*

(A and B) Intracellular IFN-γ is measured in IL-2 or IL-15-cultured NK cells from WT (n=3) and *Mirc11*$^{-/-}$ (n=3) mice after co-cultured with indicated target cell lines in E: T ratio of 1: 1.

(C) Quantitative analyses of cytokines and chemokines produced by WT (□, n=6)) or *Mirc11*$^{-/-}$ (■, n=6)) NK cells following activation with plate-bound antibodies to NKG2D, NCR1, CD137, CD244, and Ly49H receptors and in response to IL-12 and IL-18.

(D) Venn diagram demonstrating the number of genes that are differentially expressed (FDR < 0.05) in non-stimulated and anti-NKG2D mAb activated *Mirc11*$^{-/-}$ (n=3) NK cells compared to their corresponding WT (n=3) and the overlapping between those two gene sets from total RNA-seq analyses.

(E) Volcano plot demonstrating the overall alterations in the transcriptome of NK cells from *Mirc11*$^{-/-}$ (n=3) compared to WT (n=3) mice. The orange/red dots represent genes that are significantly increased, while the aqua/dark blue dots represent genes that are significantly decreased in *Mirc11*$^{-/-}$ NK cells compared to the corresponding WT counterparts. We plotted all the genes with $-\text{Log}_{10}$ (p values) greater than 80 at the Y-axis equal to 80.

(F) Heatmap derived from RNA-seq of IL-2-cultured NK cells from WT (n=3) and *Mirc11*$^{-/-}$ (n=3) that were stimulated with anti-NKG2D mAb. Shown are genes of chemokines and cytokines derived from NK cells.

Bar graphs represent the mean with the standard deviations. We analyzed the data using unpaired t-test (p-value<0.05 = *, < 0.01 = **, <0.001 =***).

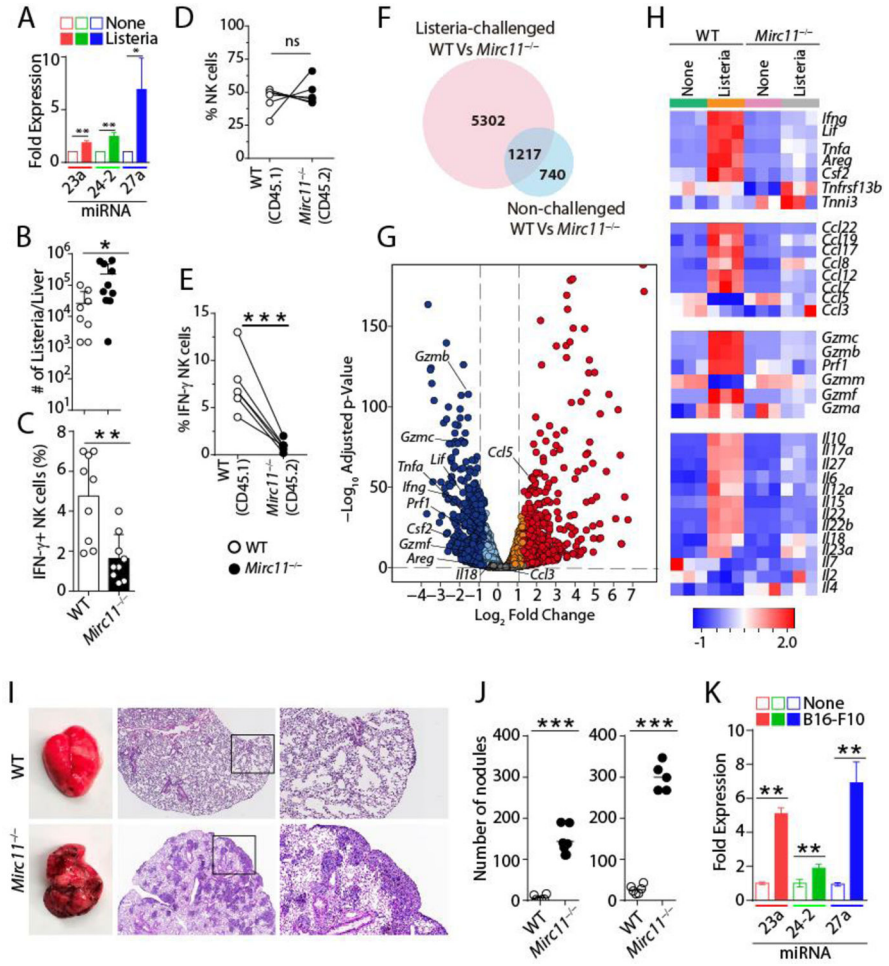

Figure 2. *Mirc11* cluster is obligatory for NK cell-mediated *in vivo* clearance of *Listeria monocytogenes*

(A) Relative expression of members of the *Mirc11*$^{-/-}$ cluster (*miR-23a*, *miR-27a*, and *miR-24-2*) expression in NK cells from the WT mice (n=3) following *L. monocytogenes* infection.

(B) WT (n=9) and *Mirc11*$^{-/-}$ (n=9) mice were infected with 2 × 10^4 CFU of *L. monocytogenes*, and 96 hours later spleens were harvested to quantify IFN-γ production in NK cells using flow cytometry.

(C) Quantification of bacterial burden in the liver indicates an inability of *Mirc11*$^{-/-}$ mice (n=9) to clear *L. monocytogenes* compared to WT mice (n=9). Bacterial burden from individual mice is shown.

(D and E) Mixed bone marrow chimerism demonstrates a cell-intrinsic role for the *Mirc11* cluster. Bone marrow cells from WT (CD45.1$^+$) and *Mirc11*$^{-/-}$ (CD45.2$^+$) mice were mixed in equal ratio and injected into irradiated *Rag2*$^{-/-}$ $\gamma_c^{-/-}$ mice (n=5). Five weeks later, mice were infected with 2 × 10^4 CFU of *L. monocytogenes*. 48 h later spleens were harvested and analyzed for total NK cells number (D) and percent IFN-γ$^+$ NK cells (E) by flow cytometry among NK cells from WT (NK1.1$^+$CD3$^-$ CD45.1$^+$) or *Mirc11*$^{-/-}$ mice (NK1.1$^+$CD3$^-$ CD45.2$^+$).

(F) Venn diagram demonstrating the number of genes that are differentially expressed (FDR < 0.05) in freshly isolated NK cells from *Mirc11*$^{-/-}$ mice (n=3) with or without *L. monocytogenes* infection compared to fresh NK cells from infected and non-infected WT mice (n=3).

(G) Volcano plot demonstrating the overall alterations in the transcriptomic profiles of NK cells from *Mirc11*$^{-/-}$ (n=3) compared to that of WT mice (n=3). The orange/red dots represent genes that are significantly increased, while the aqua/dark blue dots represent genes that are significantly decreased in NK cells from *Mirc11*$^{-/-}$ compared to the corresponding WT mice. We plotted all the genes with $-\text{Log}_{10}$ (p values) greater than 80 at the Y-axis equal to 80.

(H) RNA-seq heat map analyses of freshly isolated NK cells from *Mirc11*$^{-/-}$ mice with (n=3) or without (n=3) *L. monocytogenes* infection compared to their corresponding WT controls (n=3,3). Shown are transcripts of cytokines and chemokines either produced by or relevant to NK cells functions.

(I) Pulmonary pseudometastases in the lungs following the intravenous injection of 2×10^5 B16F10 melanoma cells in the recipient mice. Left panels, freshly isolated, one representative lung of WT (n=4) and *Mirc11*$^{-/-}$ (n=4) mice, isolated 11 days following tumor challenge. Middle panels, Hematoxylin and Eosin-stained lung sections from WT and *Mirc11*$^{-/-}$ mice. Right panels, magnified portions of lung sections shown in the middle panels (magnification, 100×).

(J) Quantification of lung nodules in tumor-challenged mice. WT (n=6) and *Mirc11*$^{-/-}$ (n=8) mice were injected intravenously with either 2×10^5 or 10^6 B16F10 cells, and the lungs were harvested 14 or 7 days, respectively. Double-blinded counting was employed to quantify the total number of tumor nodules in the lung lobes of each mouse, which are shown.

(K) Relative expression of members of the *Mirc11* cluster (*miR-23a*, *miR-27a*, and *miR-24-2*) in NK cells isolated from lungs of WT mice (n=3) challenged with 2×10^5 B16F10 melanoma cells.

The data presented is a compilation of three independent experiments showing the mean with standard error. Data were analyzed using unpaired t-test (p-value < 0.05 = *, < 0.01 = **, < 0.001 =***). Mann-Whitney U-test was used for statistical analyses of bone marrow chimerism.

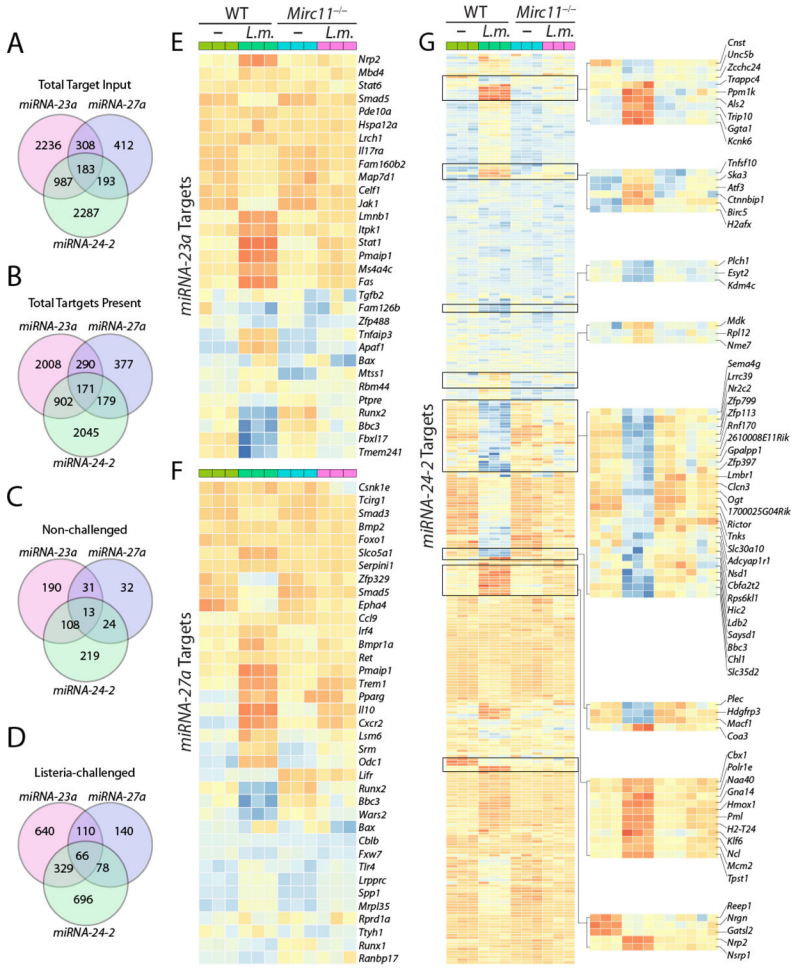

Figure 3. Qualitative alterations in the potential target transcripts of *Mirc11* cluster

(A) Venn diagram demonstrating the number of total target input that can be modulated by *miR-23a*, *miR-27a* and *miR-24-2* and the overlapping targets.

(B) Venn diagram demonstrating the number of total target genes that are expressed in NK cells and modulated by *miR-23a*, *miR-27a* and *miR-24-2* and the overlapping targets.

(C, D) Venn diagram demonstrating the number of total target genes in freshly isolated or *L. monocytogenes* challenged NK cells which can be modulated by *miR-23a*, *miR-27a* and *miR-24-2* and, the overlapping targets.

(E, F, G) Hierarchical clustering of all potential target genes of *miR-23a*, *miR-27a* and *miR-24-2* in NK cells from *L. monocytogenes* challenged mice.

TargetScan 7.1-based *in silico* analyses was used to identify the set of target mRNAs that are present in the total genome-wide RNA sequence analyses of NK cells from WT and *Mirc11*$^{-/-}$ mice that were non-challenged or challenged with *L. monocytogenes*. The algorithm to identify the targets were based on ‘the aggregate probability of conserved targeting’ (P_{CT}). *In silico* predictions that matched the 3′ UTR of the transcripts and their orthologs based on the UCSC whole-genome alignments were identified.

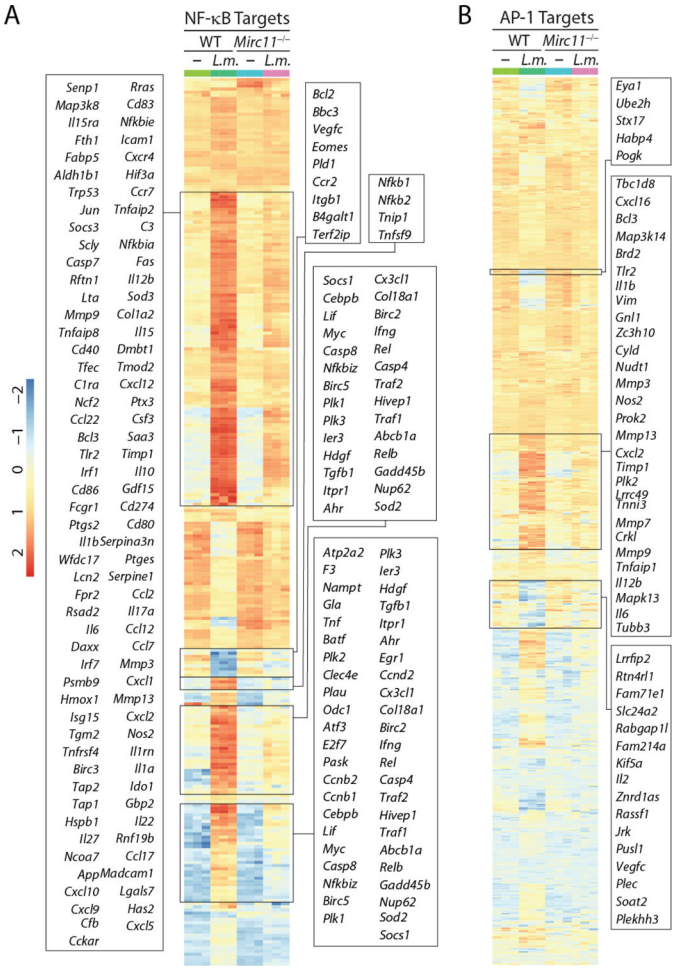

Figure 4. *Mirc11* cluster targets NF-κB and AP-1-mediated gene transcriptions

(E) Hierarchical clustering of NF-κB target genes that are differentially expressed between NK cells derived from the WT and *Mirc11*$^{-/-}$ mice using an unpaired t-test following *L. monocytogenes* infection.

(F) Hierarchical clustering of AP-1 target genes that are differentially expressed between NK cells derived from the WT and *Mirc11*$^{-/-}$ mice using an unpaired t-test following *L. monocytogenes* infection.

Gene sets were identified using IPA Informatics software through classification into gene ontology (GO) categories with a false discovery rate (FDR) of 0.01% based on biological process (BP) and molecular function (MF) categories with a minimum of two-fold change restriction. RNA-seq data from WT (n=3,3) and *Mirc11*$^{-/-}$ (n=3,3) are compared and shown.

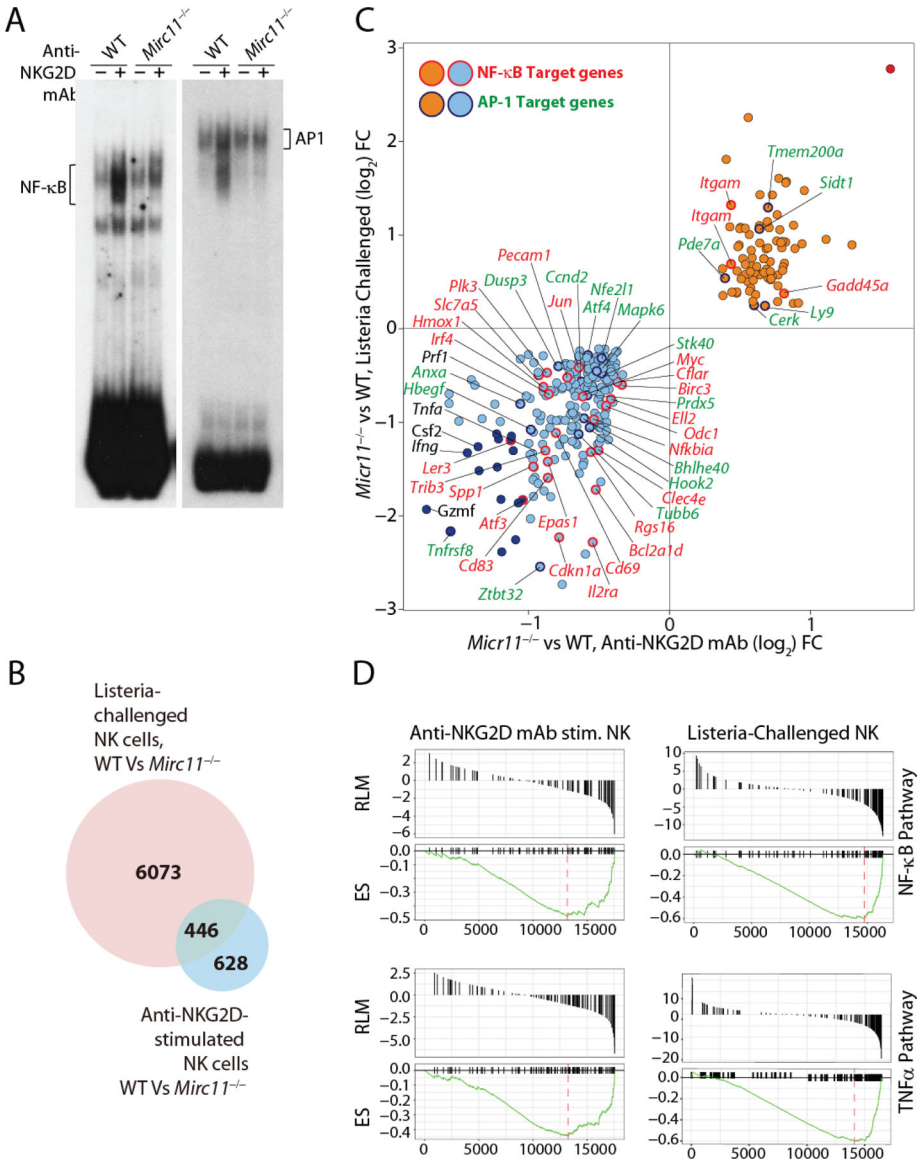

Figure 5. *Mirc11* cluster targets NF-κB and AP-1-mediated gene transcriptions

(A) Nuclear translocation of NF-κB and AP-1 were compared in NK cells derived from WT (n=3) and *Mirc11*$^{-/-}$ (n=3) mice following activation with plate-bound anti-NKG2D mAb (A10, 2.5 μg/ml). Gel-shift data presented is a representative of three independent experiments.

(B) The gene expression profiles of NK cells from *in vivo L. monocytogenes*-challenged mice (n=3,3) and *in vitro* anti-NKG2D mAb-activated (n=3,3) were compared and the number of differentially expressed (FDR < 0.05) and shared transcripts are shown in Venn diagrams.

(C) Differentially expressed known target transcripts of NF-κB and AP-1 in the absence of *Mirc11* that are shared between NK cells from *in vivo L. monocytogenes*-challenged mice (n=3,3) and in NK cells that were activated *in vitro* with anti-NKG2D mAb (n=3,3). Data is presented in a Log_2–Log_2 plot to identify shared common target transcripts. The orange/red

dots represent genes that are significantly increased, while the aqua/dark blue dots represent genes that are significantly decreased in *Mirc11*$^{-/-}$ NK cells compared to the corresponding WT counterparts. Circles with black border represent genes targeted by NF-κB and circles with red border represent genes that are targeted by AP-1.

(D) Gene Set Enrichment Analysis (GSEA) was used to show and compare the set of gene targets that are regulated downstream of NF-κB and TNF-α in NK cells that were anti-NKG2D mAb-activated (n=3,3) or NK cells derived from *L. monocytogenes*-challenged WT (n=3) and *Mirc11*$^{-/-}$ (n=3) mice.

The data presented is a compilation of three independent experiments showing the mean with standard error. Data was analyzed using an unpaired t-test (p-value < 0.05 = *, < 0.01 = **, < 0.001 =***).

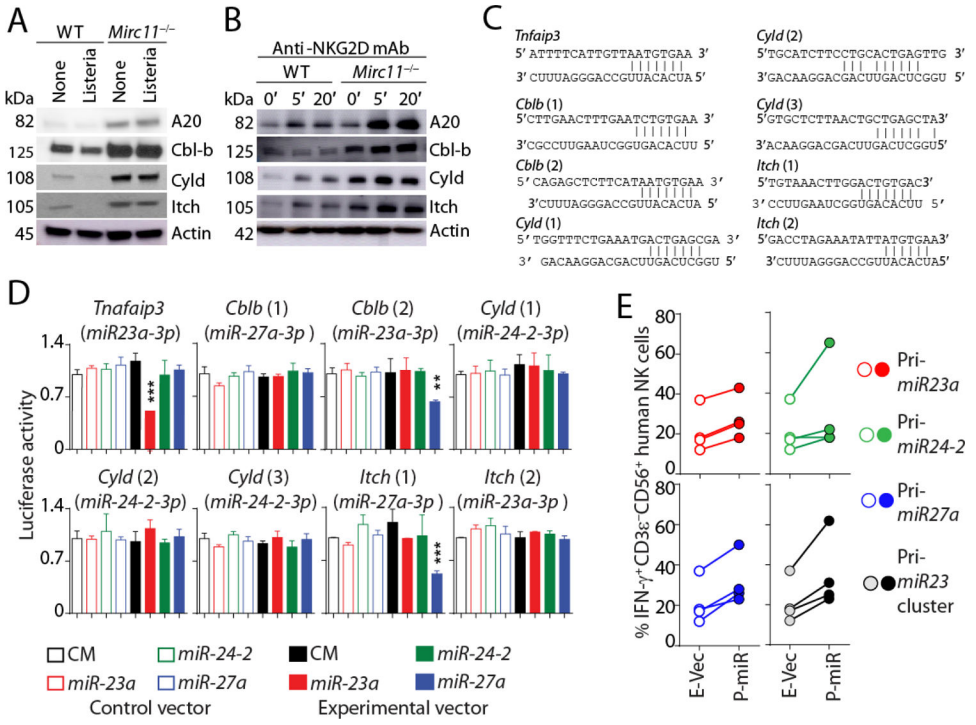

Figure 6. *Mirc11* targets members of E3 ligases in NK cells from mice and human

(A) Expression of E3 ligases A20, Cbl-b, Itch, Cyld in freshly isolated NK cells from WT (n=2) and *Mirc11*$^{-/-}$ (n=2) mice following *L. monocytogenes* infection.

(B) Expression of A20, Cbl-b, Itch, Cyld E3 ligases in IL-2-cultured NK cells from WT (n=3) and *Mirc11*$^{-/-}$ (n=3) mice following activation with plate-bound anti-NKG2D mAb at indicated time points.

(C) Predicted interactions between the 3′ UTR of transcripts encoding A20, Cbl-b, Itch, Cyld containing target sequences and the members of the *Mirc11* cluster. Sequences of target mRNA and miRNA were aligned using ‘force-directed RNA’, FORNA program available at http://rna.tbi.univie.ac.at/forna/.

(D) Dual luciferase assay measuring the activity *miR-23a*, *miR-24-2*, *miR-27a*, or control mimetics (CM) as a ratio of Renilla to Firefly luciferase on the 3’ UTR of select target genes in HEK293T cells two days after transfection. Data are normalized to the control 3’ UTR plus no miRNA condition. Transfection was done in triplicates, and the average with standard deviation is shown.

(E) Forced expression of the members of the *Mirc11* cluster in human NK cells enhances IFN-γ production. IFN-γ production by primary human NK cells transduced with pre-miR lentiviral vectors for human *miR-23a*, *miR-24-2*, *miR-27a* or CM. 48 hours following transduction NK cells were co-cultured with K562 cells, and the percent intracellular IFN-γ^{+} CD3ε^{-}CD56^{+} NK cells were enumerated. NK cells from a total of four normal healthy individuals were used.

The data presented is a compilation of three independent experiments showing the mean with standard error. Data was analyzed using unpaired t-test (p-value < 0.05 = *, < 0.01 = **, < 0.001 =***).

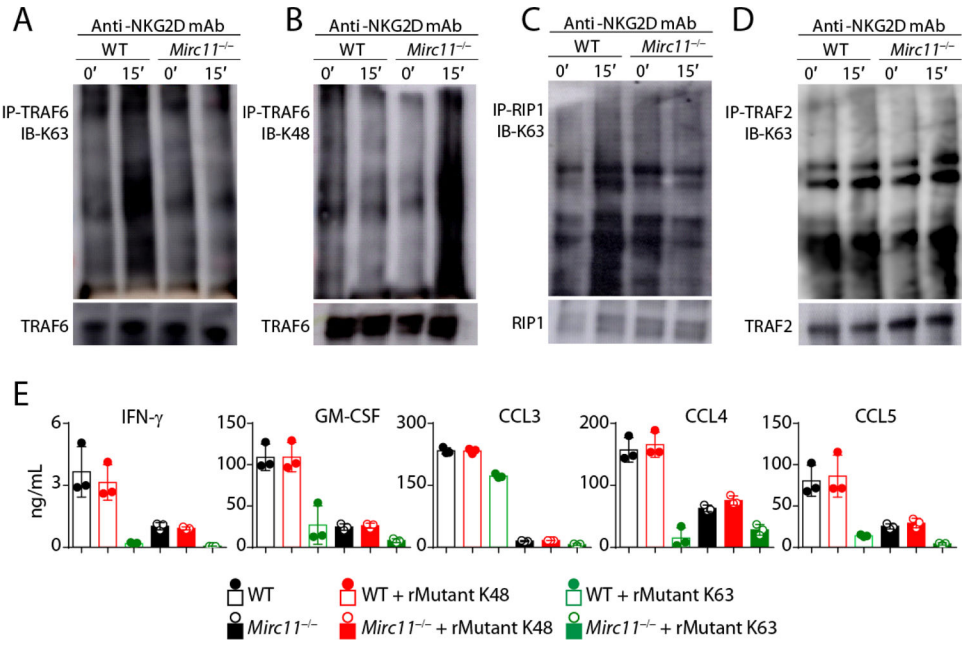

Figure 7. Lack of *Mirc11* reduces K63- and increases K48-polyubiquitination of TRAF6

(A) IL-2-cultured NK cells from WT (n=2) or *Mirc11*$^{-/-}$ (n=2) mice were activated with plate-bound anti-NKG2D mAb for 15 min, lysed, TRAF6 was immunoprecipitated, and the extent of K63 polyubiquitination was analyzed by immunoblotting.

(B) Immunoprecipitated TRAF6 was analyzed for the extent of K48 polyubiquitination was analyzed by immunoblotting (n=2).

(C) IL-2-cultured NK cells from WT (n=2) or *Mirc11*$^{-/-}$ (n=2) mice were activated with plate-bound anti-NKG2D mAb for 15 min, lysed, RIP1 was immunoprecipitated, and the extent of K63 polyubiquitination was analyzed by immunoblotting.

(D) IL-2-cultured NK cells from WT (n=2) or *Mirc11*$^{-/-}$ (n=2) mice were activated with plate-bound anti-NKG2D mAb for 15 min, lysed, TRAF2 was immunoprecipitated, and the extent of K63 polyubiquitination was analyzed by immunoblotting.

(E) IL-2-cultured NK cells from WT (n=2) and *Mirc11*$^{-/-}$ (n=2) mice were co-incubated with activated with anti-NKG2D mAb in the presence of either recombinant mutant K63 or mutant K48 ubiquitin proteins. 18 hours following activation, supernatants were analyzed for the production of indicated cytokines and chemokines.

The data is a compilation of three independent experiments plotting the mean with the error bars representing the standard error of the mean analyzing the results using unpaired t-test (p-value<0.05 = *, < 0.01 = **, <0.001 =***).